15-1231-1228

PUBLICATION OR PRESENTATION RELEASE REQUEST

Pubkey 962 NRLINST 5511.40

1. REFERENCES AND ENCLOSURES	2. TYPE OF PUBLICATION OR PRESENTATION		3. ADMINISTRATIVE INFORMATION
Ref: (a) NRL Instruction 5600.2 (b) NRL Instruction 5510.40E Encl: (1) Two copies of subject publication/presentation	( ) Abstract only, published ( ) Book author ( ) Book editor (X) Conference Proceedings (refereed) ( ) Journal article (refereed) ( ) Oral Presentation, published ( ) Video ( ) Poster	( ) Abstract only, not published ( ) Book chapter ( ) Multimedia report ( ) Conference Proceedings (not refereed) ( ) Journal article (not refereed) ( ) Oral Presentation, not published ( ) Other, explain	STRN: NRL/PP/7330-15-2545 Route Sheet No.: 7330/ Job Order No.: 73-4951-05-5 Classification: U S C FOUO Sponsor: ONR BASE 6.1-BAA Sponsor's approval: yes* (attached) (*Required if research is other an 6.1/6.2 NRL or ONR unclassified research or if publication/presentation is classified

URGENT

ALL DOCUMENTS/PRESENTATIONS MUST BE ATTACHE

4. AUTHOR

Title of Paper or Presentation

Ocean and Polarization observations from active remote sensing: Atmospheric and Ocean science applications

AUTHOR(s) LEGAL NAMES(s) OF RECORD (First, MI, Last), CODE, (Affiliation if not NRL):

DAMIEN JOSSET NRC, Weilin Hou 7333, J. Pelon IPSL/LATMOS, Y. Hu NASA/LARC - VA, S. Tanelli Jet Propulsion Laboratory, R. Ferrare NASA Langley Research Center, S. Burton NASA/LARC - VA, Nicolas Pascal ICARE Univ., ICARE team,

This paper will be presented at the SPIE DSS

(Name of Conference)

20-APR - 24-APR-15, Baltimore, MD, Unclassified

(Date, Place and Classification of Conference)

and/or for published in SPIE DSS, Unclassified

(Name and Classification of Publication) (Name of Publisher)

5. CERTIFICATION OR CLASSIFICATION

It is my opinion that the subject paper (is ____) (is not __x__) classified in accordance with reference (b) and this paper does not violate any disclosure of trade secrets or suggestions of outside individuals or concerns which have been communicated to the NRL in confidence.

This subject paper (has ____) (has never __x__) been incorporated in an official NRL Report.

Weilin Hou, 7333 (Signature)

Name and Code (Principal Author) (Legal Name of Record and Signature Only)

6. ROUTING/APPROVAL (NOTE: If name other than your legal name of record is annotated on the publication or presentation itself, add an explanatory note in the "comments" section below next to your signed legal name of record)

CODE	SIGNATURE	DATE	COMMENTS
Co-Author(s) Weilin Hou, 7333			Need by 20 Apr 2015
			This is a Final Security Review. Any changes made in the document, after approved by Code 1231, nullify the Security Review.
Section Head			
Branch Head Richard L. Crout, 7330		4-13-2015	
Division Head Ruth H. Preller, 7300		4/13/15	1. To the best knowledge of this Division, the subject matter of this publication (has ____) (has never __x__) been classified. 2. This paper (does ____) (does not __x__) contain any militarily critical technology.
ADOR/Director NCST E. R. Franchi, 7000			
~~DOR/CO~~			
Security, Code 1231		4/17/15	A copy of the paper, abstract or presentation is filed in this office.
Associate Counsel, Code 1008.3	Needs invention memo	5-8-2015	
Public Affairs (Unclassified/Unlimited Only), Code 7030.4	Shannon Mews	4-20-15	
Division, Code			
Author, Code			

HQ-NRL 5511/6 (Rev. 12/14) THIS FORM CANCELS AND SUPERSEDES ALL PREVIOUS VERSIONS

Naval Research Laboratory

Stennis Space Center, MS 39529-5004

NRL/MR/7330--15-9628

Validation Test Report for the Automated Optical Processing System (AOPS) Version 4.12

Sherwin Ladner
Richard Crout
Adam Lawson

Ocean Sciences Branch
Oceanography Division

Paul Martinolich
Jennifer Bowers

Vencore Incorporated
Chantilly, Virginia

Robert Arnone
Ryan Vandermeulen

University of Southern Mississippi
Hattiesburg, Mississippi

September 3, 2015

REPORT DOCUMENTATION PAGE

Form Approved
OMB No. 0704-0188

1. REPORT DATE *(DD-MM-YYYY)*	**2. REPORT TYPE**	**3. DATES COVERED** *(From - To)*
03-09-2015	Memorandum Report	

4. TITLE AND SUBTITLE

Validation Test Report for the Automated Optical Processing System (AOPS) Version 4.12

5a. CONTRACT NUMBER

5b. GRANT NUMBER

5c. PROGRAM ELEMENT NUMBER
06011453N

6. AUTHOR(S)

Sherwin Ladner, Richard Crout, Adam Lawson, Paul Martinolich,[a] Jennifer Bowers,[a] Robert Arnone,[b] and Ryan Vandermeulen[b]

5d. PROJECT NUMBER

5e. TASK NUMBER

5f. WORK UNIT NUMBER
73-4948-05-5

7. PERFORMING ORGANIZATION NAME(S) AND ADDRESS(ES)

Naval Research Laboratory
Oceanography Division
Stennis Space Center, MS 39529-5004

8. PERFORMING ORGANIZATION REPORT NUMBER

NRL/MR/7330--15-9628

9. SPONSORING / MONITORING AGENCY NAME(S) AND ADDRESS(ES)

Office of Naval Research
One Liberty Center
875 North Randolph Street, Suite 1425
Arlington, VA 22203-1995

10. SPONSOR / MONITOR'S ACRONYM(S)

ONR

11. SPONSOR / MONITOR'S REPORT NUMBER(S)

12. DISTRIBUTION / AVAILABILITY STATEMENT

Approved for public release; distribution is unlimited.

13. SUPPLEMENTARY NOTES

[a]Vencore Inc., 15052 Conference Center Dr., Chantilly, VA
[b]University of Southern Mississippi, 118 College Drive, Hattiesburg, MS 39406

14. ABSTRACT

Work performed under the Space and Naval Warfare Systems Center (SPAWARSYSCEN) Preparing Tactical Ocean Optical Products from Future Polar-Orbiting Sensors project enables exploitation of the Visible Infrared Imager Radiometer Suite (VIIRS) and similar ocean color sensors to provide the Navy with ocean color products to support operations. Work completed was in response to the Navy's need to exploit all available remote sensing technologies as part of a larger effort to provide a continuous operational picture of environmental conditions of the battlespace. Automated Optical Processing System (AOPS) version 4.12 provides tools and algorithms to process data from environmental remote sensing satellites and enables rapid near-real-time dissemination of final products. This Validation Test Report (VTR) provides the technical basis to transition the AOPS v4.12 to the NP3 Ocean Optics branch of the Naval Oceanographic Office (NAVOCEANO). AOPS is the software that allows NAVOCEANO to determine operational capability under various ocean optical conditions from satellite imagery. AOPS is used by NAVOCEANO to support fleet operators engaged in Naval Special Warfare (NSW), Mine Warfare (MIW), Expeditionary Warfare (EXW), and Anti-Submarine Warfare (ASW). Additionally, ocean color products are used in real time to support analysis of ocean models by oceanographers on the NAVOCEANO watch floor.

15. SUBJECT TERMS

Satellite	MODIS	Matchups	Inherent Optical Properties
Ocean color	VIIRS	Calibration	IOP
Remote sensing	GOCI	Validation	Operational

16. SECURITY CLASSIFICATION OF:			**17. LIMITATION OF ABSTRACT**	**18. NUMBER OF PAGES**	**19a. NAME OF RESPONSIBLE PERSON**
a. REPORT	**b. ABSTRACT**	**c. THIS PAGE**			Sherwin Ladner
Unclassified Unlimited	Unclassified Unlimited	Unclassified Unlimited	Unclassified Unlimited	57	**19b. TELEPHONE NUMBER** *(include area code)* 228-688-5754

Standard Form 298 (Rev. 8-98)
Prescribed by ANSI Std. Z39.18

Validation Test Report for the Automated Optical Processing System (AOPS) Version 4.12

Contents

1 Introduction

Work performed under the Space and Naval Warfare Systems Center (SPAWARSYSCEN) Preparing Tactical Ocean Optical Products from Future Polar-Orbiting Sensors project enables exploitation of the Visible Infrared Imager Radiometer Suite (VIIRS) and similar ocean color sensors to provide the Navy with ocean color products to support operations. Work completed was in response to the Navy's need to exploit all available remote sensing technologies[1] as part of a larger effort to provide a continuous operational picture of environmental conditions of the battlespace. This project was divided into four task areas, where AOPS is identified as the transitioning element of the project. As the transition, AOPS v4.12 provides tools and algorithms to process data from environmental remote sensing satellites in accordance with the Meteorology and Oceanography (METOC) Space Satellite readiness plan and enables rapid dissemination of final products via NAVOCEANO's web portal and other avenues compliant with Department of Defense (DOD) and Department of the Navy (DON) distribution policies.

This Validation Test Report (VTR) provides the technical bases to transition the Automated Optical Processing System (AOPS) version 4.12 to the NP3 Ocean Optics branch of the Naval Oceanographic Office (NAVOCEANO). AOPS is the software that allows NAVOCEANO to determine operational capability under various ocean optical conditions from satellite imagery. AOPS is used by NAVOCEANO to support fleet operators engaged in Naval Special Warfare (NSW), Mine Warfare (MIW), Expeditionary Warfare (EXW), and Anti-Submarine Warfare (ASW). Additionally, ocean color products are used in real time to support analysis of ocean models by oceanographers on the NAVOCEANO watch floor.

The AOPS collection of programs allows scientists to generate co-registered image databases of geophysical parameters derived from remotely sensed data. To accomplish this, AOPS uses the techniques of *extension* and *automation*.

Extension is the use of small programs, each designed for a specific task, and a shell to 'glue' them together. The idea is similar to the UNIX operating system and its many programs like **cat**, **tr**, **basename**, etc. and allows the user to augment the system with their own features and programs.

Automation is the technique of operating a system without human effort or decision. For AOPS, this is achieved by setting up a directory structure and using scripts to monitor the directories for new input data -- as new data is made available to the system, it is processed without user intervention.

---

[1] In light of the aging MODIS satellites and current status of the DWSS program, the Joint Polar Satellite System (JPSS) satellite and other foreign sensors (GOCI, SGLI, OLCI – Sentinel 3A) are expected to be the primary sources of DOD METOC data for the next 20 years. Naval operations will rely on the integration of these sensors into the current operational processing stream to provide continuity of legacy products and spatial coverage of current operational areas.

Manuscript approved June 30, 2015.

AOPS does not contain GUIs or visualization programs; therefore all user input *must* be provided to the program upon *start*.

2 System Description

AOPS is a collection of UNIX programs and shell scripts that enables automated generation of map-projected image data bases of satellite derived products from streaming raw satellite data. Individual scenes are sequentially processed from the raw digital counts (Level-1) using standard sensor specific parameters to a radiometrically and geometrically corrected (Level-3) product within several minutes. AOPS further processes the data into a variety of temporal composites called mosaics (Level-4). These products are stored in the Hierarchical Data Format (HDF) with specific attributes. Additionally, it automatically generates quick-look "browse" images in JPEG format.

AOPS uses a simple monitoring technique. The main driver regularly polls a specified input directory for incoming data and for each file found, executes what are known as `areas` scripts on the file in a working directory. The `areas` scripts do the actual construction of the desired results (i.e. the data bases). After each areas script has been run on the file, it is moved to an output directory. This method uses the directory as the queuing system for data to be processed.

The AOPS 4.12 version represents the most recent processing algorithms employed at the Naval Research Laboratory as of 10 Mar 2015, for current operational sensors. The system has been developed on CenTOS 5.7 (x86, x86_64) – equivalent to RHEL v5.

Historically, AOPS was capable of processing data from: Sea-viewing Wide Field-of-view Sensor (SeaWiFS), Moderate Resolution Imaging Spectrometers (MODIS on Aqua), and Medium Resolution Imaging Spectrometer (MERIS). This VTR documents the new capability in AOPS to produce operational products from the Joint Polar Satellite System (JPSS) – Suomi National Polar-orbiting Partnership (NPP) with the VIIRS sensor package as well as data from the Geostationary Ocean Color Imager (GOCI) sensor, aboard the Communication Ocean and Meteorological Satellite (COMS) satellite. Additionally, this upgrade includes improved operational products from the MODIS and VIIRS sensors that result from NASA L2gen improvements, vicarious calibration/gain updates and specific algorithm improvements requested by NAVOCEANO.

The 4.12 version was released on 10 March 2015. A list of upgrades follows:

1. update imgBrowse to create an image from three input products. *The -Y option may also read from three input products.*
2. update imgDiff to add ability to mask out pixels from result *using -M option*.
3. update imgMean to add ability to define the composite time frame *using the -R option.*
4. update imgMap giving it a completely new API.
   Ex: instead of taking two files (the input L2 and output L3), the argument list can take multiple input L2 files. So, imgMap L2file L3file [products...] becomes imgMap [-p products...] L3file L2file L2file L2file....
5. Two new imgMap options -p and -z. The first was added due to change in argument list. The second adds the ability to change the resolution of the image map used.
6. update libviirs to read the VIIRS imagery Scientific Data Record (SDRs) and geo-location data files.
7. n2gen is now a C++ compiled program.

8. n2gen was updated to reflect the NASA R2014.0 reprocessing codes. The NASA release is part of SeaDAS 7.1. The following changes were implemented:
    a. updated n2gen to Goddard L2gen v7.0.1 (from v6.7.1)
    b. updated bbw terms based on Zhang et al. (2009)
    c. updated GIOP algorithm (using temperature/salinity correct bbw and nw).
    d. new IOP algorithm (SWIM) iop_opt=8 (the LMI algorithm is now set with iop_opt=9).
    e. updated PAR algorithm.
    f. set input file name to realpath of ifile=. This allows input to be a symbolic link.
    g. allow glob of VIIRS data to handle multiple granules on disk.
    h. updated land mask file watermask15ARC.nc (not used by MODIS which retains usage of MOD44w.h5).
    i. updated met climatology file met_climatology_v2014.hdf.
    j. updated ozone climatology file ozone_climatology_v2014.hdf.
    k. new ancillary correction file anc_cor_file_28jan2014.nc for toms-like ozone with new anc_cor_file= keyword in n2gen.
    l. updated NO2 climatology file no2_climatology_v2013.hdf.
    m. new elevation file ozone_climatology_v2014.hdf with new elev= keyword in n2gen.
    n. all parameters used by n2gen which are identical across all sensors now reside in data/common/msl12_defaults.dat
    o. updates to MODIS SST processing
    p. product definitions have been removed from n2gen and placed into an XML file data/common/products.xml
    q. new VIIRS cross-calibration file n2gen. This calibration performs a detector-to-detector corrections ("de-stripping").
9. Updated MODIS Vicarious Calibration, *technique discussed in the Appendix, Section 9.3.*

Table 1 provides calibration coefficients for the MODIS sensor for AOPS v4.12**. The calibration was based on data collected at the MOBY site from June 2012 to June 2014. Validation of these coefficients was completed August 2014.**

MODIS Channel	Calibration Coefficient
412 nm	0.9748
443 nm	0.9875
469 nm	1.0173
488 nm	0.9921
531 nm	0.9995
547 nm	1.0003
555 nm	1.0003
645 nm	1.0259
667 nm	0.9988
678 nm	0.9975
748 nm	0.9989
859 nm	1.0254
896 nm	1.0000
1240 nm	1.0000
1640 nm	1.0000
2130 nm	1.0000

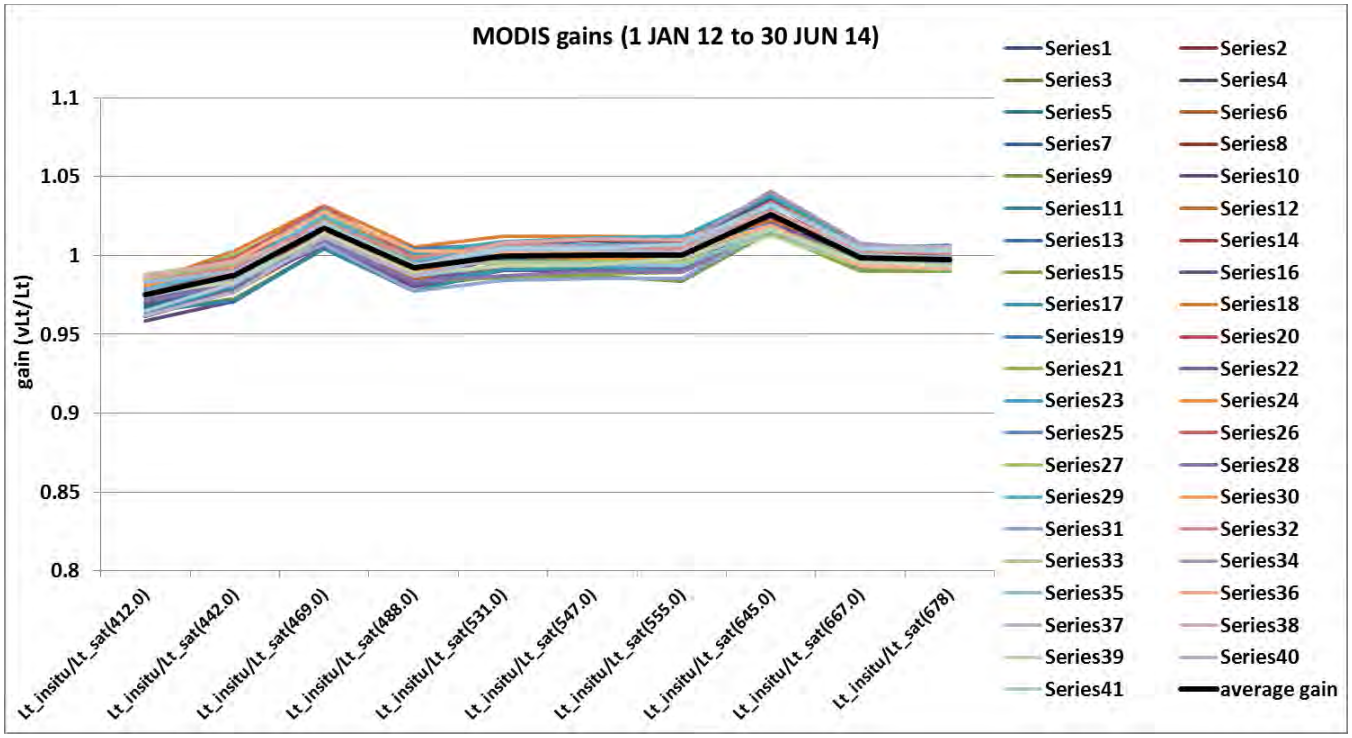

Figure 1 shows the individual gains that contribute to the MODIS vicarious calibration (average gain). Forty one matchups from 1 Jan 2012 to 30 Jun 2014 were of sufficient quality to use for calibration.

10. Updated VIIRS Vicarious Calibration. *The Vicarious Calibration procedure is discussed in the Appendix, Section 9.3.*

Table 2 provides calibration coefficients for the VIIRS sensor for AOPS v4.12**. The calibration was based on data collected at the MOBY site from June 2012 to November 2014, n = 38. Validation of these coefficients was completed December 2014.**

VIIRS Channel	Calibration Coefficient
410 nm	0.9711
443 nm	0.9769
486 nm	0.9729
551 nm	0.9564
671 nm	0.9587
745 nm	0.9800
862 nm	1.0000

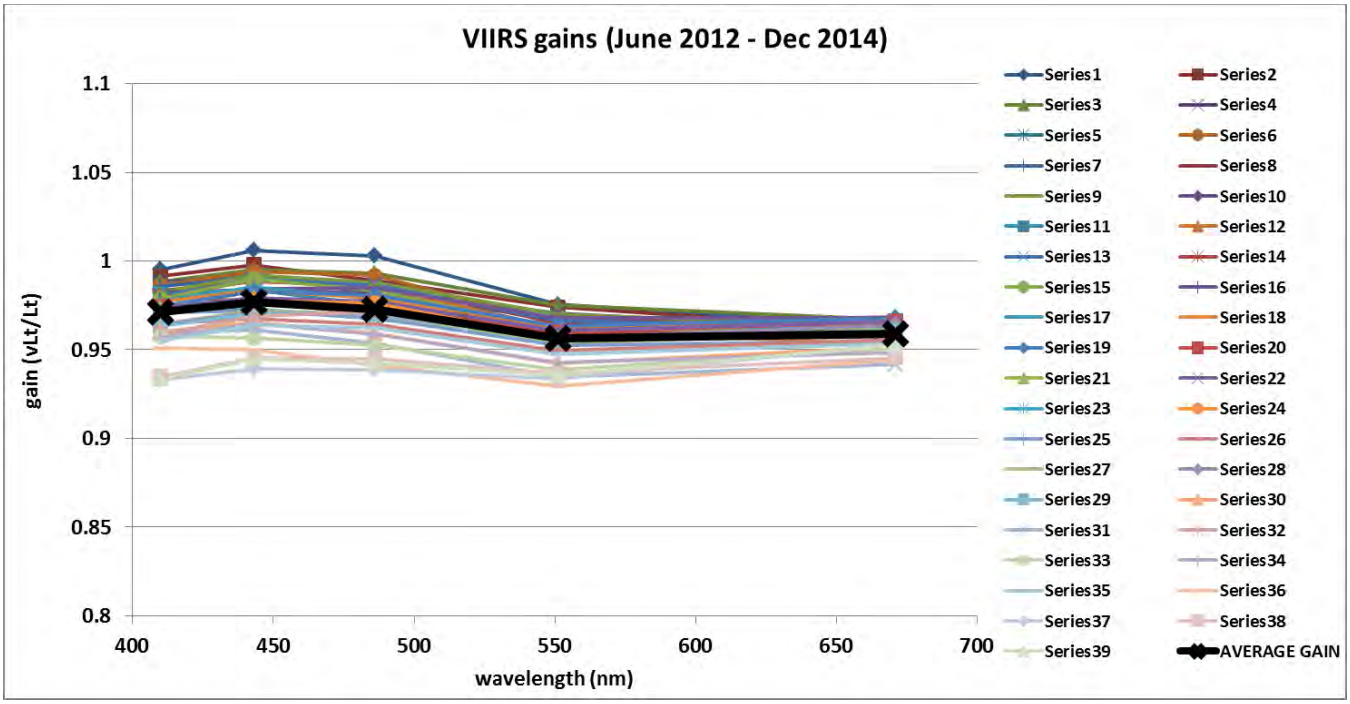

Figure 2 shows the individual gains that contribute to the VIIRS vicarious calibration (average gain). Thirty nine matchups from 1 Jan 2012 to 30 Jun 2014 were of sufficient quality to use for calibration.

11. Updated GOCI Vicarious Calibration. *The Vicarious Calibration procedure is discussed in the Appendix, Section 9.3.*

Table 3 provides calibration coefficients for the GOCI sensor for AOPS v4.12**. The calibration was based on data collected from the MODIS sensor from the GOCI_CalSite_1 from 2011 to 2014, n = 20. Validation of these coefficients was completed September 2014.**

GOCI Channel	Calibration Coefficient
412 nm	0.9676
443 nm	0.9530
490 nm	0.9173
555 nm	0.8786
660 nm	0.8807
680 nm	0.8580
745 nm	0.9430
862 nm	1.0000

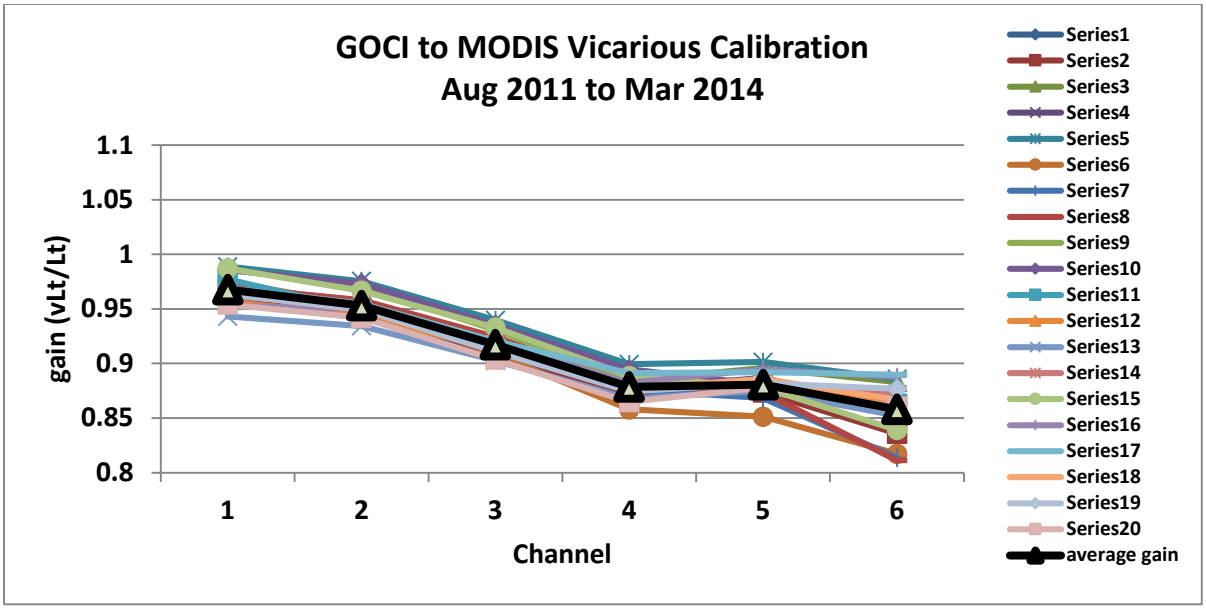

Figure 3 shows the individual gains that contribute to the GOCI vicarious calibration (average gain). Twenty matchups were of sufficient quality to use for calibration. This is calibration is a sensor to sensor adjustment where we force GOCI as best as practicable to match MODIS. The GOCI gains will be monitored with respect to MODIS until sufficient matchups are available to support traditional ground truth based Calibration/Validation (Cal/Val) techniques.

12. Maps has new option mercator designed to simplify the creation of Mercator maps.
13. All area scripts now have a single entry point apsProcessFile. This replace the sensor specific versions (modProcess, ...)
14. The processing variable DayOnly is now defined and set to "yes". It is no-longer required in the area scripts.
15. Processing variables have been generalized. So, ModLPCompOpts has been changed to LPCompOpts in all area scripts.
16. A new program apsArea has been implemented. This program consolidates all the other related programs into a single executable. Therefore, modArea, viirsArea, etc. no longer exist.
17. In Addition, the apsArea program has a new option -B which allows the user to define a bounding box for the input map. When present, this option will cause apsArea to extract any attributes that the input file might have to quickly determine if the file covers the map. For example, the VIIRS data files include an attribute North_Bounding_Coordinate which is read and tested against the -B values. If the input does not have any bounding coordinate attributes, apsArea will run as normal.
18. All area scripts have set of bounding values which are used by the SGE master to quickly test files for map coverage.
19. The SGE master script apsSGE.sh has been updated to use the new apsArea program. It uses the bounding coordinates to quickly test files for coverage on region.
20. The apsSGE.sh also automatically tests for day-time only MODIS and VIIRS processing to speed up standard processing.
21. The apsSGE.sh has been updated to handle VIIRS imagery band inputs (375m data) and GOCI data.
22. The apsSGE.sh has been updated to automatically remove invalid symbolic links in input directory.
23. All area scripts now have a post-processing call to multi_sensor_composite. This script combines the data from VIIRS and MODIS into a single file to enhance operational support capability.
24. All area scripts now produce the chlor_a product (OCI). This new algorithm is from Hu, et. al. and is the new NASA standard. It replaces the O'Reilly, et. al. polynomial chl_oc3m product.

25. All area scripts which made a sub-image based on latitude and longitude now use the imgBrowse geographical bounding box option. With this option, the North-South-West-East bounds are used.

2.1 System Requirements

AOPS runs in the Red Hat Enterprise Linux (RHEL) environment. Users should be familiar with UNIX; BASH shell programming; and remote sensing -- particularly regarding computer processing of satellite data. System memory and storage requirements are difficult to gauge. The amount of memory needed is dependent upon the amount and type of satellite data needed to be processed; the larger the area, the larger the memory requirement. For example, the entire Atlantic Ocean will require more processing power than the Mississippi Bight. In addition, the type of data being processed will determine how robust the supporting system should be. Data storage requirements are a function of the temporal and spatial needs of both the NAVOCEANO system operators and the data consumers. A technical description for how to use AOPS that would enable identification of memory and disk space requirements is provided in the AOPS Users Guide v4.12, 2015 (http://www7333.nrlssc.navy.mil/docs/aops_v4.12/html/user/aps.xhtml).

2.1.1 Data Input

Currently AOPS supports VIIRS inputs provided by the Air Force Weather Agency (AFWA) stream delivered to NAVOCEANO. A redundant data stream is available through National Oceanic and Atmospheric Administration's (NOAA) Comprehensive Large Array-data Stewardship System (CLASS). At the time of this writing the data sources are identical therefore after establishing data subscriptions, processing is transparent.

The GOCI inputs are provided to NAVOCEANO from the Korea Ocean Research and Development Institute (KORDI). Additionally GOCI data can be obtained from http://www.ioccg.org/sensors/GOCI.html.

2.1.2 AOPS Output

The AOPS format is based on the Scientific Data Sets interface in version 4 of the Hierarchical Data Format (HDF4). No other interface or objects are used or allowed in a valid AOPS file.

Within the Scientific Data Sets subset, a valid AOPS file is limited to an array of no more than three dimensions one of which may be UNLIMITED. All standard number types (INT8, UINT8, INT16, UINT16, INT32, UINT32, FLOAT32, FLOAT64, and CHAR8) may be used.

None of the pre-defined attributes using such API's as SDgetdatastrs(), for example, are used. The AOPS format supports both file and data set attributes. The AOPS format has several required file and data set attributes that must exist with each file or data set, respectively.

There is no limit to the number of data sets other than those imposed by the HDF4 library. However, there are some limits placed on the names of general data set names.

The AOPS IO library contains routines for accessing all objects from the AOPS file. Use of this library is strongly encouraged as the underlying file structure may change. The AOPS User's Guide v4.12, 2015 describes the file format structure as well as the use of the library.

2.1.2.1 Level 3 Regional Data Products

AOPS generates radiometrically and geometrically corrected (Level-3) products in a Hierarchical Data Format Release 4 (HDF4) format within several minutes. There are a *variable* number of data sets in an AOPS Level-3 Regional Data Product file. The *metadata sets* are standard, providing geographical coverage and data quality information. The p*roduct data sets* contain the actual geophysical products and vary in number. A long descriptive name is used to facilitate use of the p*roduct data sets*, and in some cases, the algorithm used is also provided in the name. Examples are "Remote Sensing Reflectance at 443 nm" and "Chlorophyll Concentration, OC4 Algorithm". File attributes are associated with all products in the HDF4 file. Additional output file types supported include: version 5 of the HDF format (using HDF5 v1.8.6) and the netCDF v4. The attributes are divided into several groups and a detailed discussion can be found in the AOPS v4.12 Users Guide, 2015.

2.1.2.2 Level-4 Regional Data Products

AOPS also generates several different temporal composites (Level-4) in the HDF4 format. The Level-4 Regional Data Product File contains atmospherically corrected geophysical products in a standard map projection for a specific region of interest derived from one of several operational satellites (GOCI, MODIS, and VIIRS). A Level-4 Regional Data Product may be stored in one of several formats. The default is stored using HDF4 developed by the National Center for Supercomputer Applications (NCSA) at U. of Illinois Urbana-Champaign (version 4.2.8). Additional output file types that are supported include: version 5 of the HDF format (using HDF5 v1.8.6) and the netCDF v4. A technical description can be found in the AOPS v4.12 Users Guide, 2015.

3 Validation Test Descriptions

The VTR for AOPS v4.12 describes the testing and data comparisons necessary to demonstrate the products derived from the VIIRS sensor can be used to support naval operations and should be integrated into NAVOCEANO operations to support the fleet.

Traditional *ground truthing* with *in situ* observations is one of two approaches employed to evaluate the MODIS, VIIRS and GOCI ocean color products. Satellite sensor products are compared to *in situ* ocean color data collected at the MOBY site and the WaveCIS and IEODO sites from the Aerosol Robotic Network – Ocean Color (AERONET-OC), as well as available oceanographic cruise data collection.

The second approach for evaluating ocean color products is done by inter-sensor comparison between NPP-VIIRS, MODIS and GOCI. This cross-platform approach will enable consistent data sets from which global sensor metrics of the satellite products can be established. Additionally, cross-platform calibration will allow validation of products in critical coastal regions where *in situ* data is not readily available.

We will demonstrate the operational capability of AOPS by showing:

- The improvement provided by the upgrades in AOPS v. 4.12 as compared to AOPS V 4.10. *For a list of improvements, refer to Section 2 System Description of this document.*
- Traditional ground truth via matchups of satellite ocean color products with *in situ* data collection in open ocean (blue water) and coastal (green water) environmental conditions.
- Inter-sensor comparisons provide a direct comparison with existing satellite products, *enabling cross-platform capability.*
- The effects of a procedure for the spatial enhancement of VIIRS ocean color products using sharpening.
- The effects of updates on the Linear Matrix Inversion technique by comparison of diver visibility products.
- The new image merge capability allowing enhanced spatial coverage by combining the individual images from two sensors.

Product Validation

Satellite ocean color is used to determine water quality properties, however, this requires that the sensor is well characterized and calibrated, and that processing adequately addresses the atmospheric correction to derive radiometric water leaving radiance (nLw). Radiometric properties are then used to retrieve products such as chlorophyll, optical backscattering and absorption. The JPSS ocean calibration and validation program for VIIRS establishes methods and procedures to insure the accuracy of the retrieved ocean satellite products and to provide methods to improve algorithms and characterize the product uncertainty. Initial results were presented for the VIIRS ocean color products including inter-comparisons with satellite and *in situ* observations by Arnone et al., 2012. Significant follow on validation has been performed by members of the JPSS Cal/Val team; recent work includes *but is not limited to*: Ondrusek, et al. 2014, Bowers, et al. 2014, Wang et al. 2014, Arnone, et al. 2014, Ladner et al. 2014, Pahlevan et al., 2013, Arnone et al., 2013, Davis et al. 2013, Ahmed et al. 2013.

For this analysis, validation was performed with minimal screening criteria applied to provide a more operational testing scenario. Matchup data were limited to within 3 hours with typical *in situ* screening. The satellite was selected as a single pixel unless specifically noted otherwise. The standard exclusionary angles were used, removing viewing angles above 56 degrees and 70 degrees for the satellite and solar zenith angles, respectively. Level 2 quality flags were used to remove records affected by atmospheric failure, navigation failure, clouds/ice, land, high LT, high glint. After accounting for exclusion criteria and processing techniques, the *in situ* data was directly compared to the satellite data to validate the coastal algorithm and track satellite performance over time.

Inherent optical properties (IOP) and other follow on products are derived from the remote sensing reflectance and water leaving radiance products. Generally there are two accepted approaches for extracting bio-geophysical information from remotely sensed data. Empirical algorithms generally use waveband ratios of upwelling or normalized water-leaving radiance or remote sensing reflectance. Coefficients for these algorithms are generally derived by global and seasonal pooling of data collected at a variety of temporal and spatial scales. This approach removes “noise” associated with the data sets but diminishes the spatial and temporal features of the global waters. Alternatively semi-analytical

algorithms are based on the spectral $b_b/(a+b_b)$ to remote sensing reflectance relationship. By taking a physics based approach, improved products will become available as research allows however it is essential to recognize development of these algorithms remains a work in progress[2]. For the general oceanographer not familiar with optics, IOP retrievals are difficult and often reflect the limitations of the algorithms rather than stand as a statement regarding satellite performance. As a baseline, literature suggests that mean relative errors ranging from 30 – 70% for IOP retrievals are not uncommon in coastal waters (Chang and Gould, 2006, Ladner, et al. 2002).

3.1 Gain monitoring at MOBY

To assess system stability for MODIS and NPP-VIIRS, we monitor the top of the atmosphere (TOA) radiance as predicted by MOBY *in situ* measurement to the satellite measured TOA, measured with no calibration adjustment (unity gains). This is the only data set where we employ strict calibration quality screening, allowing only the ocean flag and restricting angles, etc. as defined by NASA OBPG methodology (Baliey et al. 2008, Franz et al., 2007). Figure 4 shows the VIIRS gain (vLt/Lt) over time at MOBY site using unity gain coefficients. In a perfect system in which all components are computed accurately, the vicarious TOA radiance (vLt) and satellite TOA radiance (Lt) should have a ratio of 1.0. Most of the ratios are below the 1.0 line suggesting the sensor without vicarious calibration is slightly high. The mean gain set for the 412, 442, 490, 555, and 668 channels were determined to be 0.9711, 0.9769, 0.9729, 0.9564, and 0.9587 respectively. The data also show the satellite continues to require periodic calibration updates as a stable system would exhibit no trend.

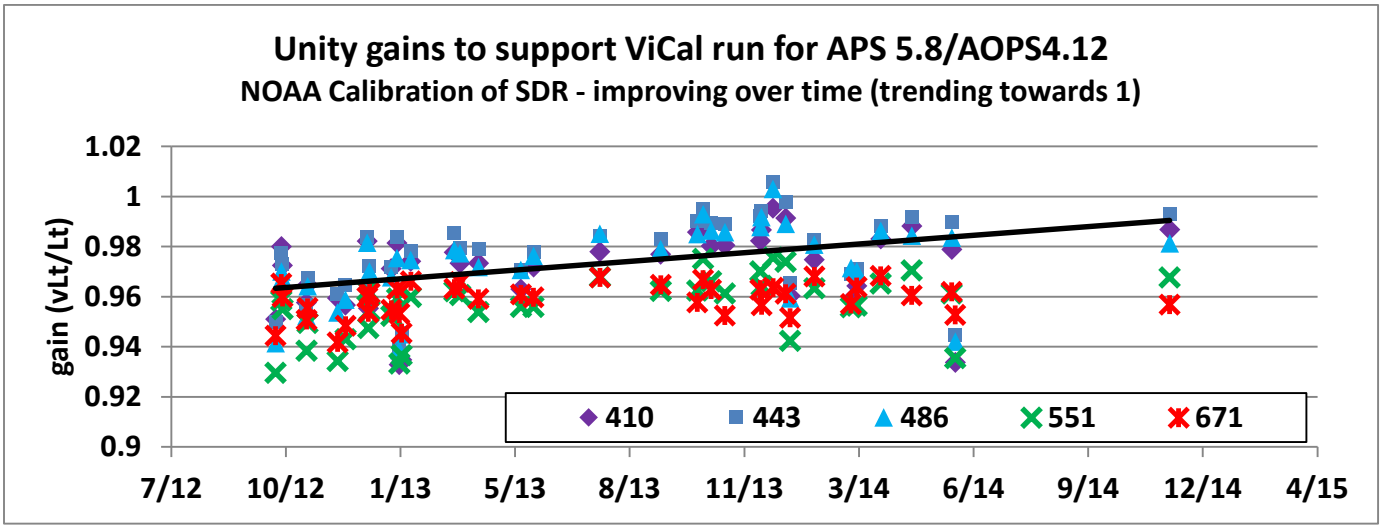

Figure 4 shows the VIIRS gain (vLt/Lt) over time at MOBY site using unity gain coefficients. In a perfect system in which all components are computed accurately, the vicarious TOA radiance (vLt) and satellite TOA radiance (Lt) should have a ratio of 1.0. Most of the ratios are below the 1.0 line suggesting the sensor without vicarious calibration is slightly high. The mean gain set for the 412, 442, 490, 555, and 668 channels were determined to be 0.9711, 0.9769, 0.9729, 0.9564, and 0.9587 respectively. The data also show the satellite continues to require periodic calibration updates as a stable system would exhibit no trend.

[2] A through discussion of deriving IOPs from remote sensing can be found in the IOCCG Report 5, 2006.

3.2 AOPS v4.12 to v4.10 comparisons

In order to compare the newly upgraded AOPS v4.12 to the current operational AOPS v4.10 we provide image to image comparisons in the Gulf of Mexico (GOM) and compare the satellite imagery with data supplied from the MOBY site.

3.2.1 Image to Image Comparison

The AOPS v4.12 *upgrades are detailed in Section 2 System Description.*

Figure 5 shows the MODIS aqua and VIIRS chlorophyll products from the 25 Oct 2014 image from the Northern Gulf of Mexico. The top images were processed with AOPS v4.10 and the bottom images were processed with AOPS v4.12; *MODIS imagery on the left and VIIRS on the right*. The most significant change in the VIIRS imagery is the de-striping provided by the L2gen cross-calibration upgrade with the secondary effect of reproducing the higher offshore values as seen in the MODIS.

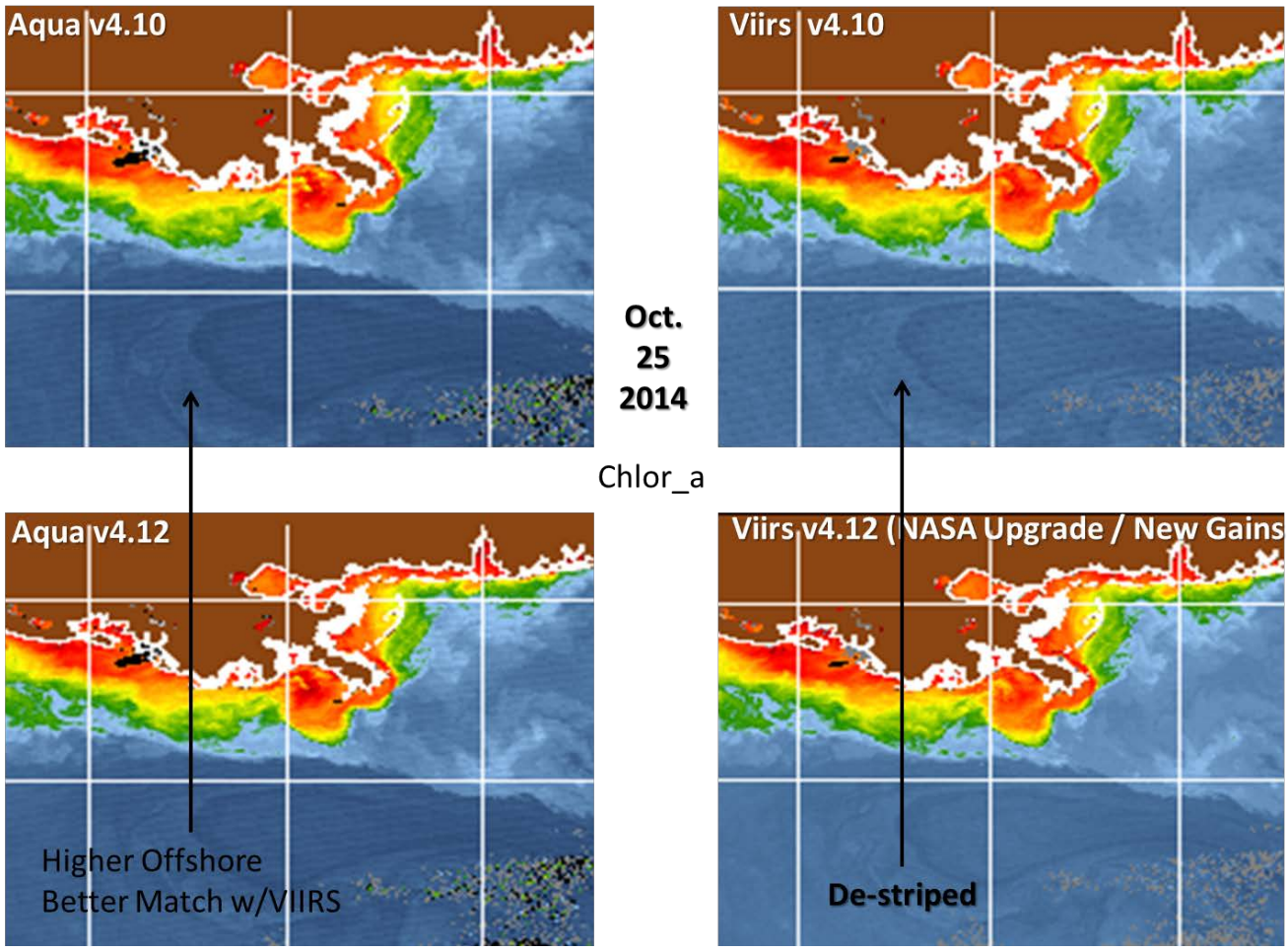

Figure 5 shows the MODIS aqua and VIIRS chlorophyll products from the 25 Oct 2014 image from the Northern Gulf of Mexico. The top images were processed with AOPS v4.10 **and the bottom images were processed with AOPS** v4.12**;** ***MODIS imagery on the left and VIIRS on the right.*** **The most significant change in the VIIRS imagery is the de-striping provided by the L2gen cross-calibration upgrade with the secondary effect of reproducing the higher offshore values as seen in the MODIS.**

3.2.2 Image to Ground Truth (MOBY) Comparison

In order to quantify the upgraded performance of AOPS v4.12 we utilize a quality control procedure called Pareto Analysis[3]. This technique shows us the relative frequency of error distribution over a determined time period of satellite performance. The Pareto chart has 2 parts: a bar graph and frequency distribution curve. The lengths of the bars represent frequency of matchups (y-axis) within a known error, i.e. *% change from the in situ reading at MOBY (x-axis).* This gives a visual depiction of where the errors are occurring. A Cumulative Frequency is then calculated by normalizing the frequency within each bin to the total number of matchups.

This comparison only utilized data collected from June 2012 to Dec 2014, because significant improvements were implemented in the Scientific Data Record (SDR) / Level-1B process from November 2011 to May 2012. By beginning our analysis at June 2012, we remove some of the uncertainty due to instability from the SDR. Matchups are satellite to MOBY high quality (Q2) and images with high glint or atmospheric complications are not considered.

Figure 6 shows the Pareto analysis for the M1 matchups of AOPS v4.12 VIIRS nLw at 410nm at MOBY. For each satellite to *in situ* matchup pair from June 2012 to Dec 2014, we calculated the % change from the *in situ* point and display the frequency of occurrences within a given error range (5%, 10%, 15%, 20%, 30%, 40%, 50% and greater than 50%), represented by the blue bars. For example, there are 13 matchups within 5% of the MOBY measurement over the time period. To generate the Cumulative % curve, normalize the result by the total number of samples over the time period 13/37 = 35.14%. Therefore for *AOPS* v4.12, 35% of the data is within 5% of the ground truth. The cumulative frequency curve shows that 92% of the satellite data is within 20% of the MOBY at the M1 channel.

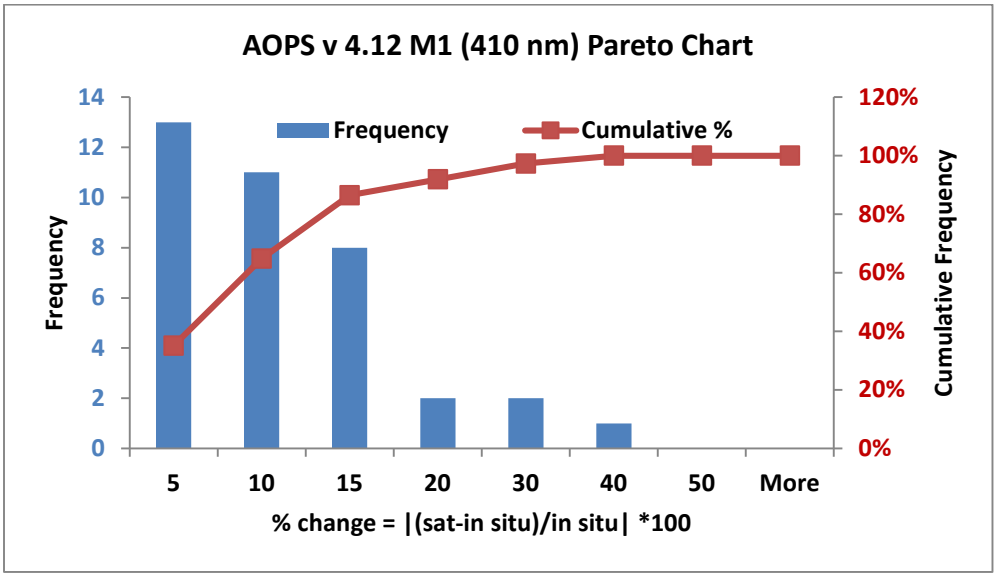

Figure 6 shows the Pareto analysis for the M1 matchups of AOPS v4.12 **VIIRS nLw at 410nm at MOBY. For each satellite to *in situ* matchup pair from June 2012 to Dec 2014, we calculated the % change from the *in situ* point and display the frequency of occurrences within a given error range (5%, 10%, 15%, 20%, 30%, 40%, 50% and greater**

[3] See Appendix 9.2

than 50%), represented by the blue bars. For example, there are 13 matchups within 5% of the MOBY measurement over the time period. To generate the Cumulative % curve, normalize the result by the total number of samples over the time period 13/37 = 35.14%. Therefore for *AOPS* v4.12, 35% of the data is within 5% of the ground truth. The cumulative frequency curve shows that 92% of the satellite data is within 20% of the MOBY at the M1 channel.

The Pareto charts are generated for all VIIRS wavelengths for both versions of AOPS (v4.12 and v4.10) at MOBY site. To compare the new software to the old, we look at the results of the cumulative frequency relative to processing version. Figure 7 shows cumulative frequency curves from the Pareto analysis for AOPS v4.12 and AOPS v4.10 for VIIRS nLw @410nm at MOBY site. Notice the AOPS v4.12 (blue line) is higher than the AOPS v4.10 (red). The higher point/curve indicates the system with better performance within a given error bin. AOPS v4.12 has 35% of its data within 5% of the ground truth while AOPS v4.10 23% of its retrievals within 5% of truth. AOPS v4.12 outperforms v4.10 up until the 20% error level, where the cumulative performance begins to level out. In other words, AOPS v4.12 has a larger number of matchups with less error than the previous version, AOPS v4.10.

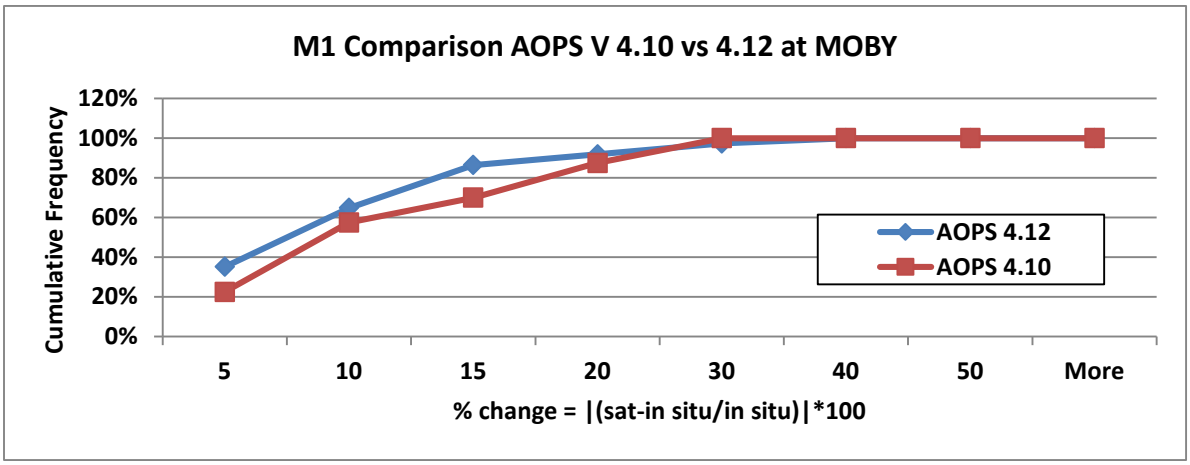

Figure 7 shows cumulative frequency curves from the Pareto analysis for AOPS v4.12 and AOPS v4.10 for VIIRS nLw @410nm at MOBY site. Notice the AOPS v4.12 **(blue line) is higher than the AOPS v4.10 (red). The higher point/curve indicates the system with better performance within a given error bin. AOPS v4.12 has 35% of its data within 5% of the ground truth while AOPS v4.10 23% of its retrievals within 5% of truth. AOPS v4.12 outperforms v4.10 up until the 20% error level, where the cumulative performance begins to level out. In other words, AOPS v4.12 has a larger number of matchups with less error than the previous version, AOPS v4.10.**

Figure 8 shows the cumulative frequency curves for AOPS v4.12 and v4.10 for remaining VIIRS spectral channels M2 – M5 at MOBY site. *The higher the point and or curve (higher frequency with lower uncertainty) indicates better performance within an error bin.* For most channels AOPS v4.12 outperforms AOPS v4.10. The M4 channel shows that at the 10 % change from *in situ*, v4.10 results are slightly better however when taken as a whole, AOPS v4.12 demonstrates the performance lead at the 15% (and greater) of ground truth with 57% of the data within that error bin. Of interest is the M5 (671nm) channel has a different shape when compared to M1 – M4 results. This indicates that the errors in the red channel are significantly greater than the other wavelengths, but is not unexpected due to the low signal to noise ratio for both the satellite and *in situ* sensor at this channel.

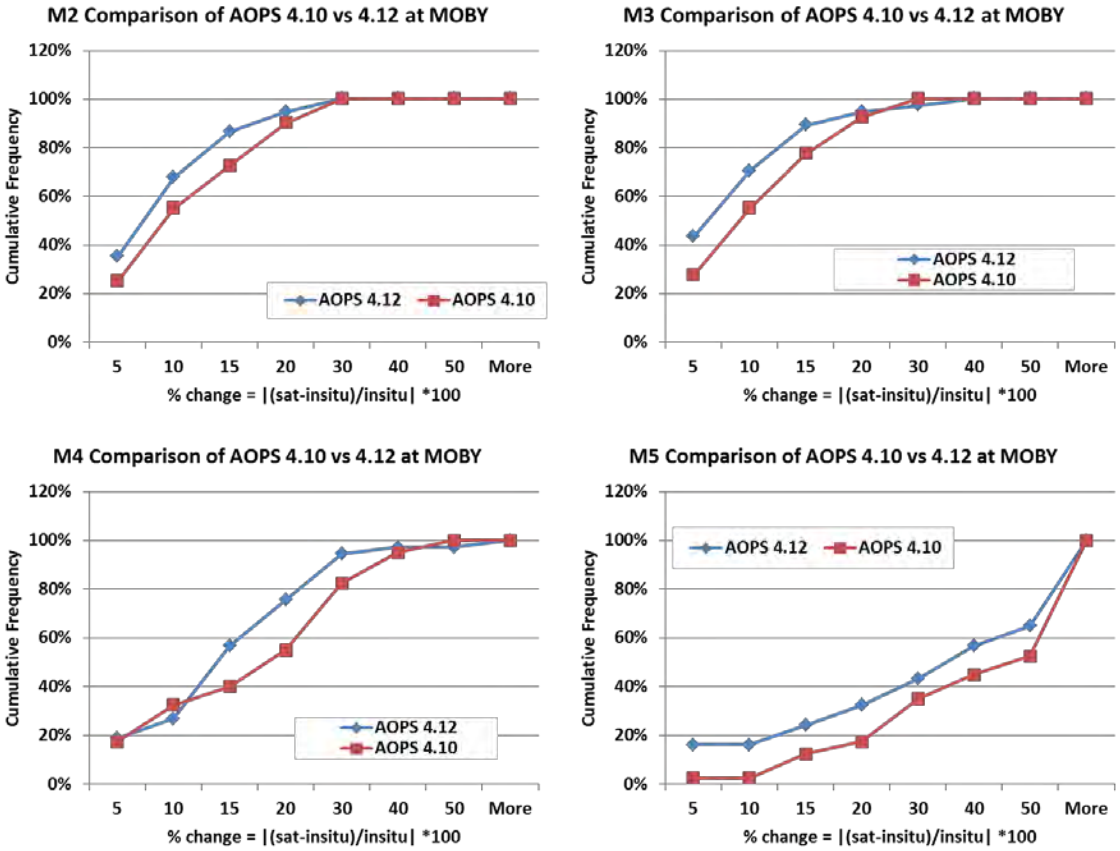

Figure 8 shows the cumulative frequency curves for AOPS v4.12 and v4.10 for remaining VIIRS spectral channels M2 – M5 at MOBY site. *The higher the point and or curve (higher frequency with lower uncertainty) indicates better performance within an error bin.* For most channels AOPS v4.12 outperforms AOPS v4.10. The M4 channel shows that at the 10 % change from *in situ*, v4.10 results are slightly better however when taken as a whole, AOPS v4.12 demonstrates the performance lead at the 15% (and greater) of ground truth with 57% of the data within that error bin. Of interest is the M5 (671nm) channel has a different shape when compared to M1 – M4 results. This indicates that the errors in the red channel are significantly greater than the other wavelengths, but is not unexpected due to the low signal to noise ratio for both the satellite and *in situ* sensor at this channel.

3.3 Matchup Analysis

This section describes the effect of updated calibration coefficients and system processing on the nLw retrievals and a variety of derived products including IOPs and chlorophyll in blue and green water regimes. Following standard practice, MOBY data is used to validate the blue water. The AERONET-OC and cruise data demonstrate AOPS v4.12 capabilities in the green water regime. This VTR utilizes data from the AERONET-OC stations in the Gulf of Mexico (WaveCIS) and Yellow Sea (IEODO).

3.3.1 Blue Water: MOBY

MOBY is a NOAA-funded project that provides data for vicarious calibration of ocean color satellites (Clark, et al. 2003). The buoy is located in the waters off Lanai, Hawaii, in 1200 m of water. Since late 1996, it has provided the primary basis for the on-orbit vicarious calibration for the United States, European, and Japanese satellites. The data from this site supports vicarious calibration of individual sensors and international efforts to develop a global, multi-year time series of consistently calibrated

ocean color data products. MOBY data is currently available in real time, with uncertainty estimates of approximately 5% for MODIS channels 8 through 12 and 12.5% for channel 13, *due to a large shadowing correction* (Brown et al., 2007).

We looked at overall trends of the VIIRS ocean color matchups as compared to the ground truth collected by the MOBY buoy. The objective was to ascertain that VIIRS is able to capture the overall trend of spectral nLw as compared to ground truth and identify issues that need to be resolved.

We assembled a data set of Level 2 (L2) matchups from the NRL SAVANT SQL database and web site of spectral VIIRS nLw retrievals and their corresponding nearest in time *(+/- 3 hours), in situ* measurements from the MOBY buoy. *All satellite retrievals were processed using the NRL APS v5.8 ViCal.rb script, which provides the same processing capability as AOPS v4.12.* The matchup data were screened using minimal data flags and constraints: atmospheric and navigation failures, high satellite and solar angles, and high to moderate glint. Validation quality screening was employed to reflect a more operational scenario[4]. The data set consisted of 122 coincident nLw retrievals at MOBY from Jun 2012 to Dec 2014.

Time series are created for each spectral channel to determine if the VIIRS retrievals are reproducing the ground truth signal. Figure 9 shows the time series for the 410 nm (M1) channel. The satellite clearly captures the trend of nLw at MOBY from Jun 2012 to Dec 2014. All spectral plots indicated the same results, where the satellite:*in situ* trend was evident, with few outliers; therefore linear regression analysis was performed to investigate how well the satellite compared to the ground truth. The following five figures summarize the results where Figure 10 shows the 410 nm (M1) nLw regression for the satellite (VIIRS) and *in situ* data from the MOBY site from 1 Jun 2012 up to 31 Dec 2014. Matchups are minimally screened, removing: negative values at any wavelength, extreme viewing angles, glint, clouds, navigation failures, atmospheric failures. A red 1:1 line is provided for reference. The regression and correlation coefficients indicate a tight correlation (close to 1) between the satellite and *in situ* sensors. The remaining spectral channels M2 – M5 are summarized respectively by Figure 11 through Figure 14.

[4] The assumption is that NAVOCEANO will use whatever data is available at any given time to support operations, regardless of if the data collection meets stringent calibration criteria. Assembling enough top-quality data to support calibration can take up to a year at the MOBY site.

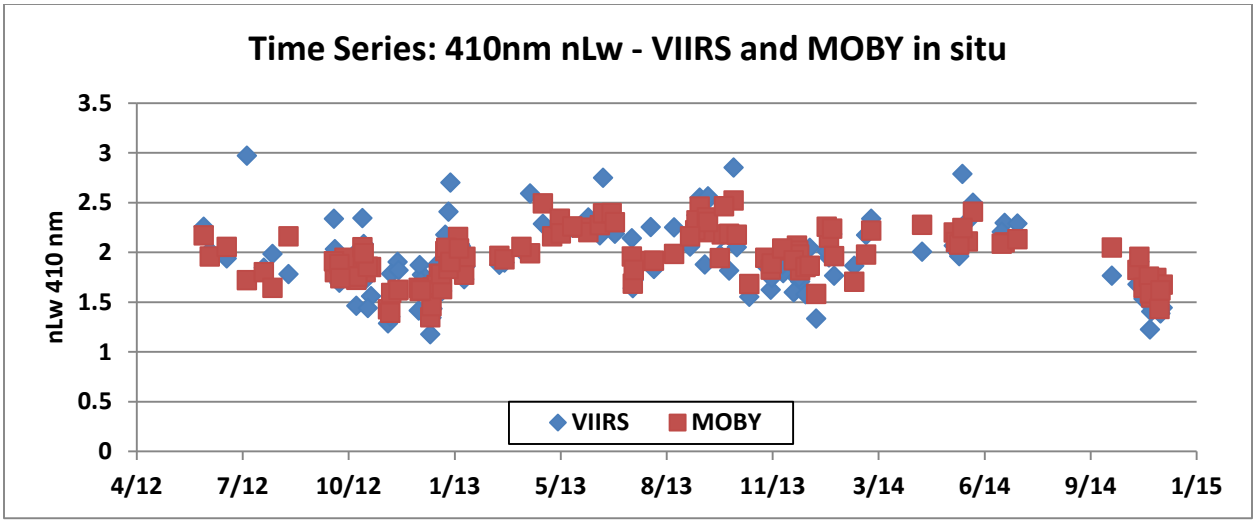

Figure 9 shows the time series for the VIIRS M1 (410 nm) channel plotted with the *in situ* value taken by the MOBY buoy. The satellite clearly captures the trend of nLw at this station over the time period. The satellite data (n = 122) is only screened for atmospheric and navigation failures, high satellite angles, and glint, therefore outliers are expected. Less stringent screening was intentionally employed to provide more of an operational description of the data.

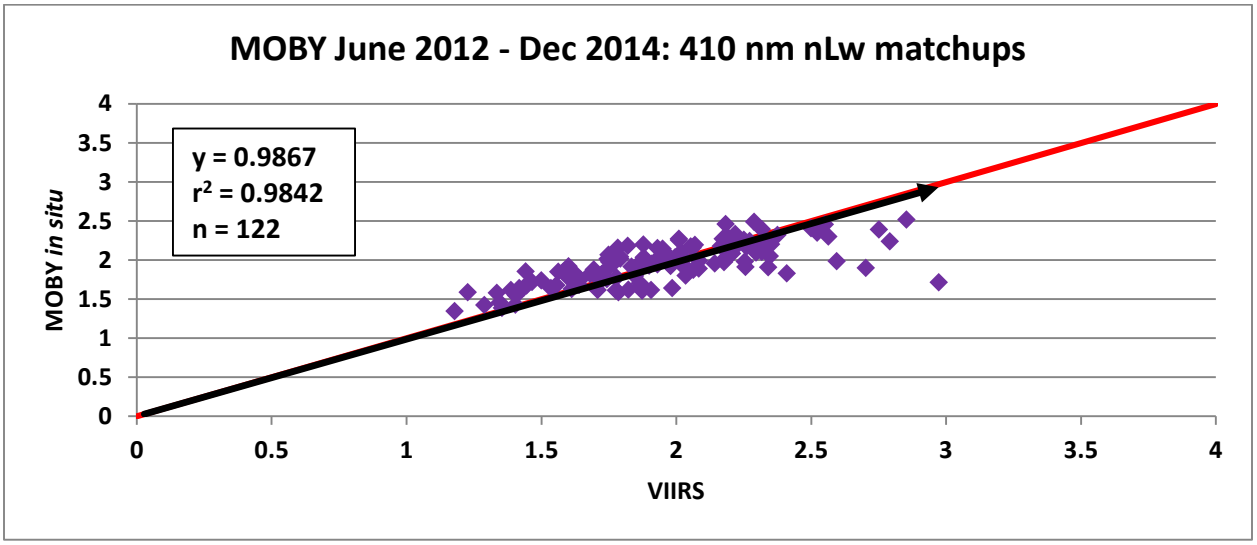

Figure 10 shows the 410 nm (M1) nLw regression for the satellite (VIIRS) and *in situ* data from the MOBY site from 1 Jun 2012 up to 31 Dec 2014. Matchups are minimally screened, removing: negative values at any wavelength, extreme viewing angles, glint, clouds, navigation failures, atmospheric failures. A red 1:1 line is provided for reference. The regression and correlation coefficients indicate a tight correlation (close to 1) between the satellite and *in situ* sensors.

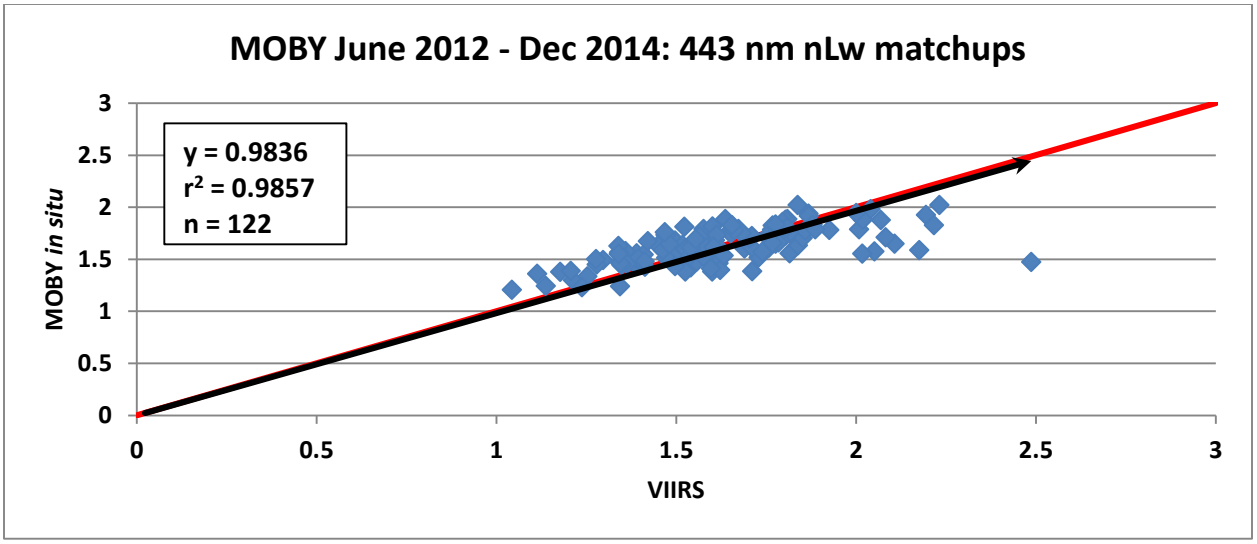

Figure 11 shows the 443 nm (M2) nLw regression for the satellite (VIIRS) and *in situ* data from the MOBY site from 1 Jun 2012 up to 31 Dec 2014. Matchups are minimally screened, removing: negative values at any wavelength, extreme viewing angles, glint, clouds, navigation failures, atmospheric failures. A red 1:1 line is provided for reference. The regression and correlation coefficients indicate a tight correlation (close to 1) between the satellite and *in situ* sensors.

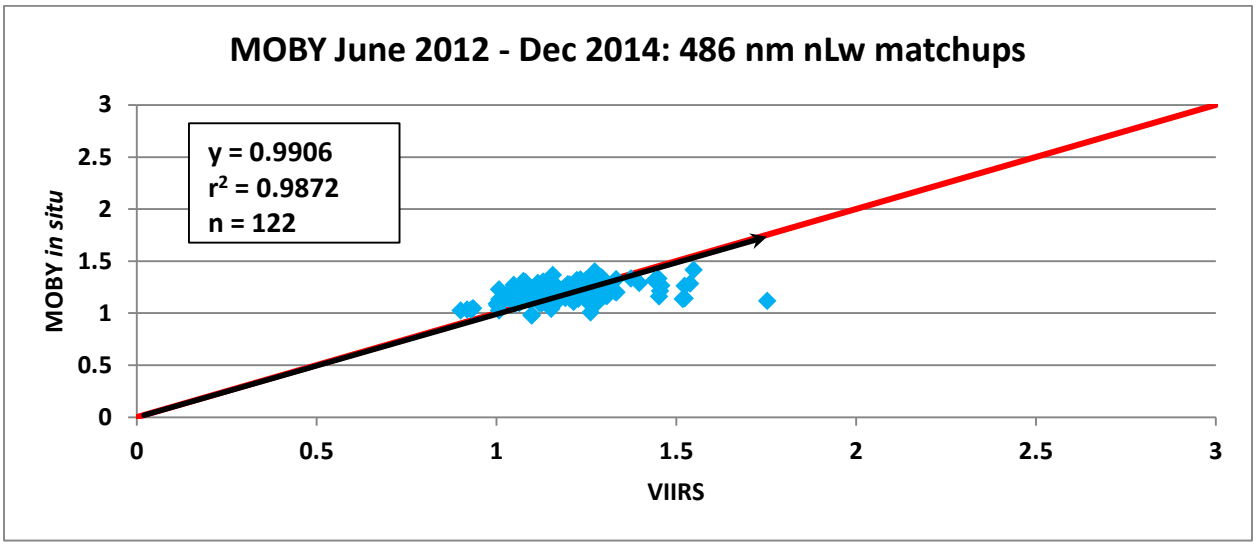

Figure 12 shows the 486 nm (M3) nLw regression for the satellite (VIIRS) and *in situ* data from the MOBY site from 1 Jun 2012 up to 31 Dec 2014. Matchups are minimally screened, removing: negative values at any wavelength, extreme viewing angles, glint, clouds, navigation failures, atmospheric failures. A red 1:1 line is provided for reference. The regression and correlation coefficients indicate a tight correlation (close to 1) between the satellite and *in situ* sensors.

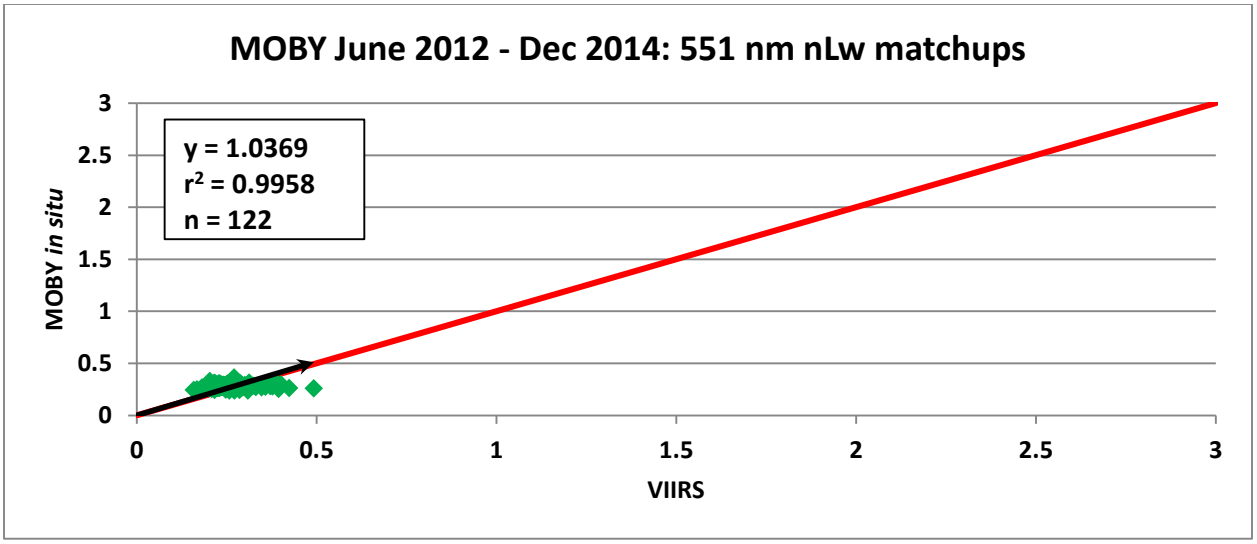

Figure 13 shows the 551 nm (M4) nLw regression for the satellite (VIIRS) and *in situ* data from the MOBY site from 1 Jun 2012 up to 31 Dec 2014. Matchups are minimally screened, removing: negative values at any wavelength, extreme viewing angles, glint, clouds, navigation failures, atmospheric failures. A red 1:1 line is provided for reference. The regression and correlation coefficients indicate a tight correlation (close to 1) between the satellite and *in situ* sensors. Notice the range of VIIRS (0.15 – 0.5) compared to the *in situ* buoy (0.25 – 0.37). The matchups are affected by natural environmental variability and uncertainty of the pixel to point matchups at these low nLw retrievals.

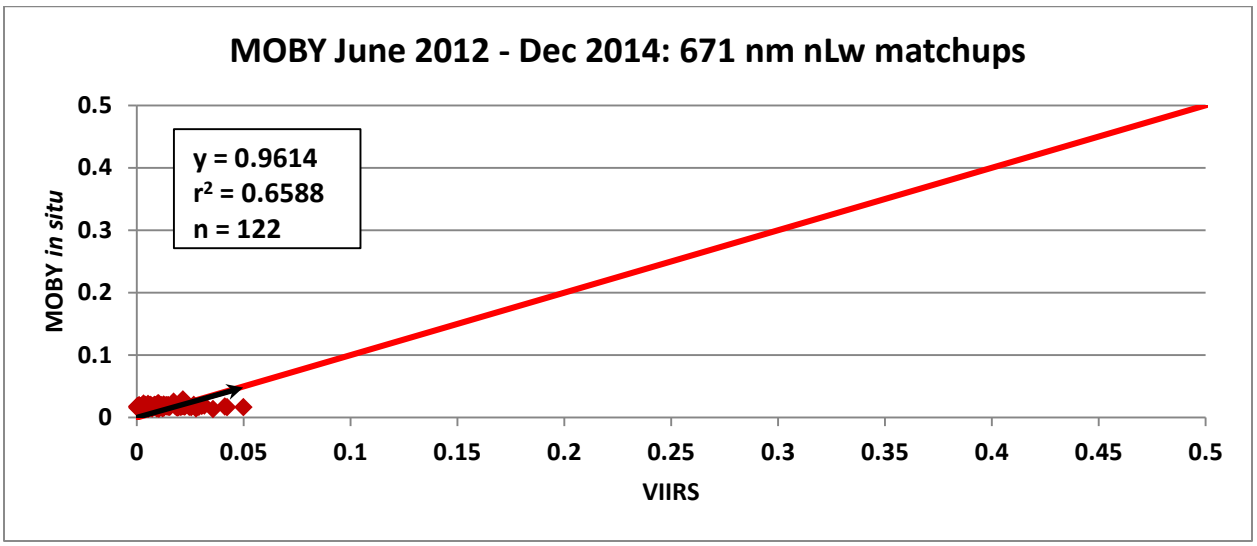

Figure 14 shows the 671 nm (M5) nLw regression for the satellite (VIIRS) and *in situ* data from the MOBY site from 1 Jun 2012 up to 31 Dec 2014. Matchups are minimally screened, removing: negative values at any wavelength, extreme viewing angles, glint, clouds, navigation failures, atmospheric failures. A red 1:1 line is provided for reference. While the regression coefficient indicates a tight correlation (close to 1) the correlation coefficient shows only moderate agreement between the sensors. It is clear by the range of VIIRS (0 – 0.05) compared to the *in situ* buoy (0.12 – 0.03) that the data is affected by signal to noise issues and the uncertainty of the pixel to point matchups. The result is neither unexpected nor alarming especially when considering the sensor to sensor comparisons in green water (*which gives higher S:N at longer wavelengths*).

3.3.2 Green Water

3.3.2.1 AERONET-OC WaveCIS

AERONET-OC is a sub-network of the Aerosol Robotic Network (AERONET)[5] using modified sun-photometers to support ocean color validation activities with standardized measurements of normalized water leaving radiance and of aerosol optical properties. Autonomous radiometers are operated on fixed platforms in coastal regions. The rational for the AERONET-OC is to validate coastal nLw retrievals from current ocean color sensors. Strict criteria exist for data collection, protocols, and processing to calculate the nLw for use in satellite product Calibration/Validation (Cal/Val) activities (Zibordi et al. 2009). To use the AERONET-OC data for near real time efforts, an intermediate product known as Level 1.5 data is utilized. An estimate of the overall uncertainty budget in AERONET-OC Lwn (Level 2) has shown values typically below 5% at the blue and green center wavelengths. Uncertainties around 8% have been estimated for the red center wavelengths (D'Alimonte and Zibordi, 2006; D'Alimonte et al. 2008; Zibordi et al. 2009). The level 1.5 data is not guaranteed at these uncertainty estimates so additional quality control is performed by persons knowledgeable in ocean optics data collection.

A similar analysis to that performed for blue water was replicated using the AERONET-OC located at the WaveCIS platform. The system is mounted on a Shell oil platform in the Gulf of Mexico and maintained by NRL thru Louisiana State University. We looked at overall trends of the VIIRS matchups compared to the ground truth collected by the WaveCIS AERONET-OC. The objective was to determine if VIIRS is able to capture the overall trend of spectral nLw as compared to ground truth (WaveCIS) and identify potential issues that need to be resolved.

The matchup data set was assembled from the NRL SAVANT SQL database and web site pairing spectral VIIRS nLw retrievals with their corresponding nearest in time *(+/- 3 hours), in situ* measurements. *All satellite retrievals were processed using the NRL APS v5.8 ViCal.rb script, which provides the same processing capability as AOPS v4.12.* The matchup data were screened using minimal data flags and constraints: atmospheric and navigation failures, high satellite and solar angles, and glint. The data set consisted of 139 coincident nLw retrievals at WaveCIS from Jun 2012 to Dec 2014.

Time series are created for each spectral channel to determine if the VIIRS retrievals are reproducing the same ground truth signal. Figure 15 shows the time series for the 410 nm (M1) channel. The satellite generally captures the trend of nLw at MOBY from Jun 2012 to Dec 2014. As compared to the MOBY 410 nm time series, WaveCIS expresses greater uncertainty in the matchups. This is expected with the complex marine atmosphere and dynamic water composition in the coastal ocean. All spectral plots show the general trend at the site is reproduced in the satellite data with a few outliers. Subsequently, linear regression analysis was performed to determine how well the satellite compared to the ground truth. The following five figures (*Figure 16* - ***Error! Reference source not found.***) summarize the results where Figure 16 shows the 410 nm (M1) nLw matchups between the VIIRS satellite and *in situ* data from the WaveCIS site from Jun 2012 to Dec 2014. Matchups are minimally screened, removing: negative values at any wavelength, extreme viewing angles, glint, clouds, navigation failures,

[5] This data is quality controlled and hosted by NASA.

atmospheric failures. A red 1:1 line is provided for reference. The regression indicates a strong correlation (close to 1) between the satellite and *in situ* sensors. Notice the correlation coefficient indicates lower strength of correlation at this wavelength as compared to MOBY (r2 = 0.9842). This is due to several factors including complex marine atmospheric conditions close to the coast and the dynamic changes in the in water constituents (particles, dissolved organic material, phytoplankton).

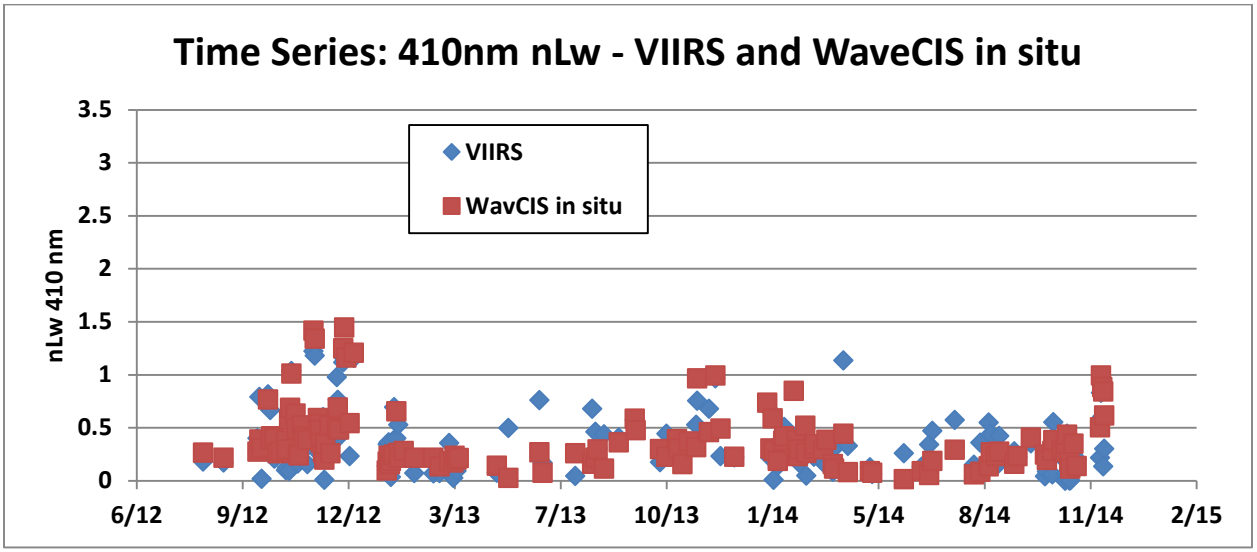

Figure 15 shows the time series for the VIIRS M1 (410 nm) channel plotted with the *in situ* value taken at WaveCIS. The satellite generally captures the trend of nLw at this station over the time period. The satellite data (n = 139) is only screened for atmospheric and navigation failures, high satellite angles, and glint, therefore outliers are expected. Less stringent screening was intentionally employed to provide more of an operational description of the data.

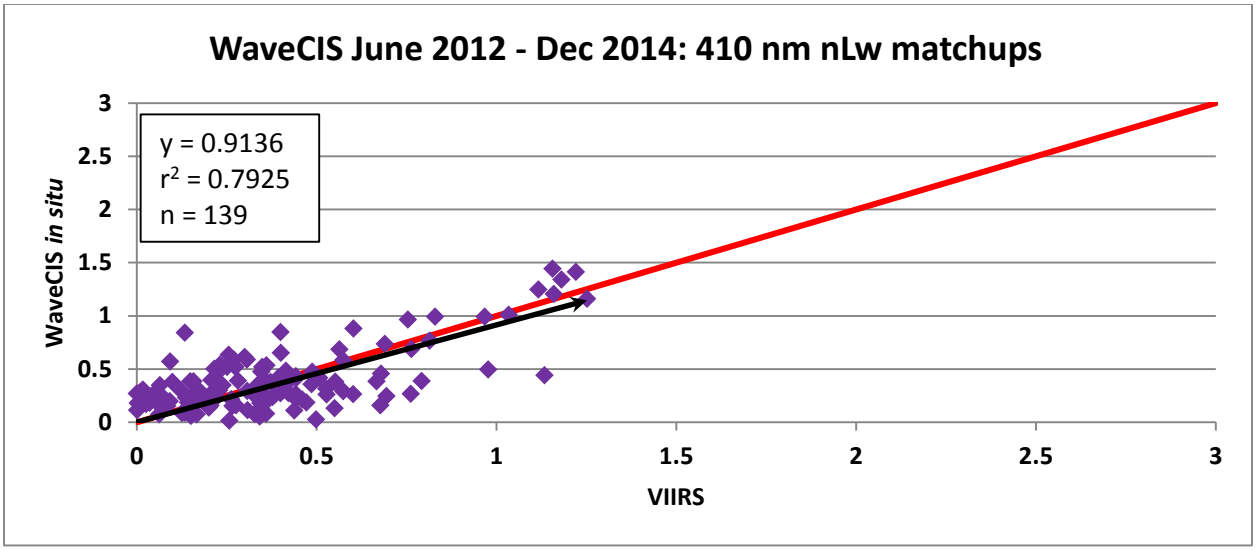

Figure 16 shows the 410 nm (M1) nLw matchups between the VIIRS satellite and *in situ* data from the WaveCIS site from Jun 2012 to Dec 2014. Matchups are minimally screened, removing: negative values at any wavelength, extreme viewing angles, glint, clouds, navigation failures, atmospheric failures. A red 1:1 line is provided for reference. The regression indicates a strong correlation (close to 1) between the satellite and *in situ* sensors. Notice the correlation coefficient indicates lower strength of correlation at this wavelength as compared to MOBY (r^2 = 0.9842). This is due to several factors including complex marine atmospheric conditions close to the coast and the dynamic changes in the in water constituents (particles, dissolved organic material, phytoplankton).

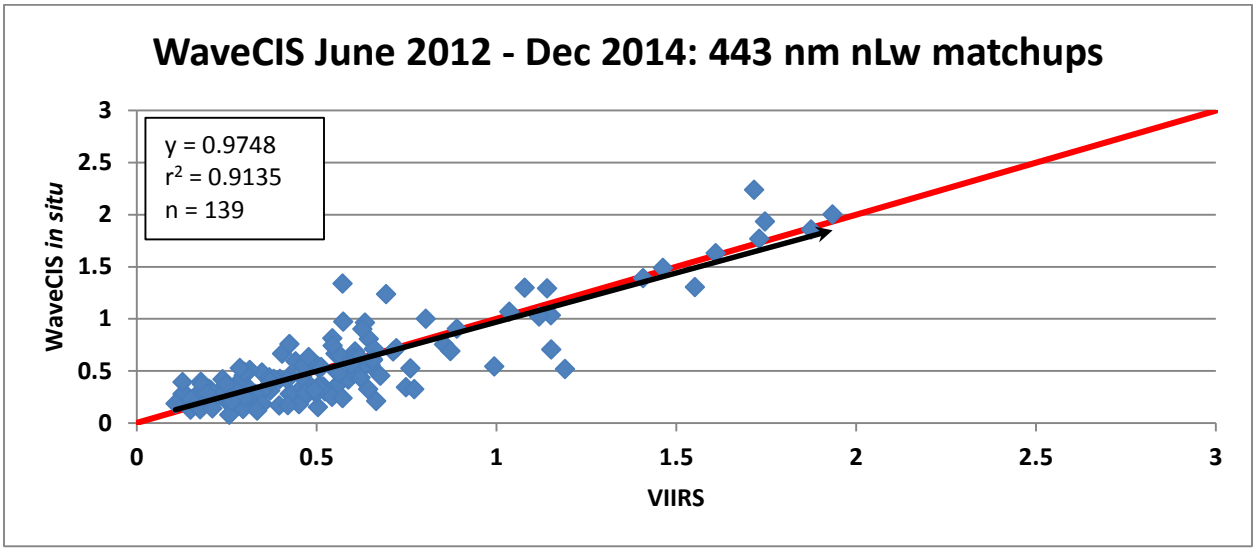

Figure 17 shows the 443 nm (M2) nLw matchups between the VIIRS satellite and *in situ* data from the WaveCIS site from 1 Jun 2012 up to 31 Dec 2014. Matchups are minimally screened, removing: negative values at any wavelength, extreme viewing angles, glint, clouds, navigation failures, atmospheric failures. A red 1:1 line is provided for reference. The regression and correlation coefficients indicate a tight correlation (close to 1) between the satellite and *in situ* sensors. Notice the correlation coefficient is lower than for the same channel than at MOBY (r^2 = 0.9857). This is due to uncertainty from the complex marine atmosphere and dynamic (time/space variance) of the in water constituents.

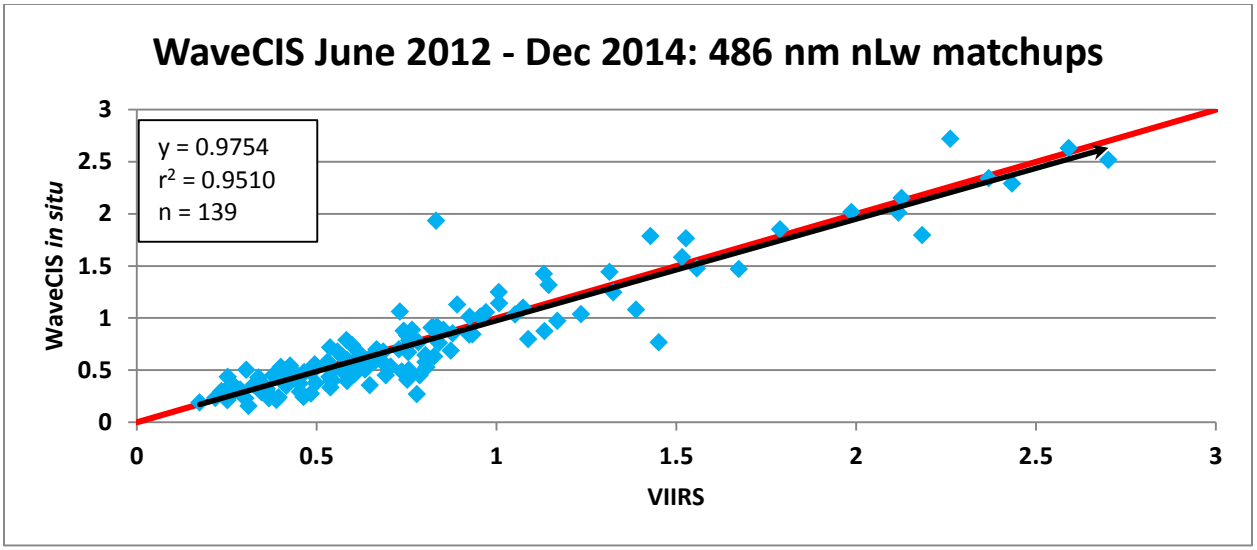

Figure 18 shows the 486 nm (M3) nLw matchups between the VIIRS satellite and *in situ* data from the WaveCIS site from 1 Jun 2012 up to 31 Dec 2014. Matchups are minimally screened, removing: negative values at any wavelength, extreme viewing angles, glint, clouds, navigation failures, atmospheric failures. A red 1:1 line is provided for reference. The regression and correlation coefficients indicate a tight correlation (close to 1) between the satellite and *in situ* sensors.

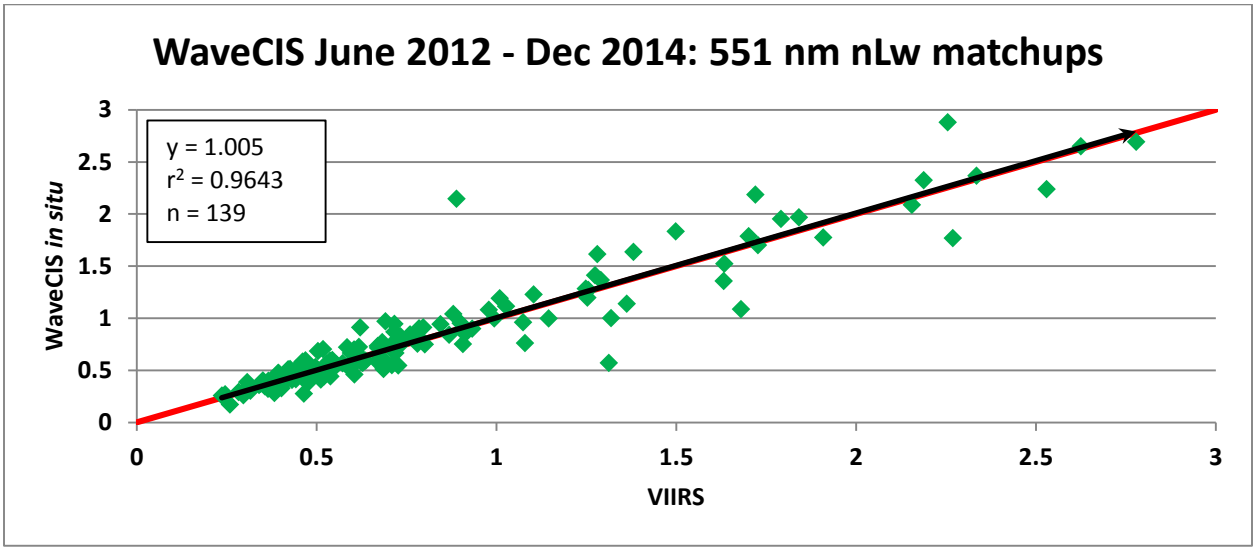

Figure 19 shows the 551 nm (M4) nLw matchups between the VIIRS satellite and *in situ* data from the WaveCIS site from 1 Jun 2012 up to 31 Dec 2014. Matchups are minimally screened, removing: negative values at any wavelength, extreme viewing angles, glint, clouds, navigation failures, atmospheric failures. A red 1:1 line is provided for reference. The regression and correlation coefficients indicate a tight correlation (close to 1) between the satellite and *in situ* sensors. Notice the range of VIIRS (0.23 – 2.8) more appropriately covers the natural range of nLw from open ocean to coastal waters, *compare to MOBY (0.15, 0.5)*. This is due to stronger reflectance of green light in the coastal waters, *effectively increases signal to noise ratio.*

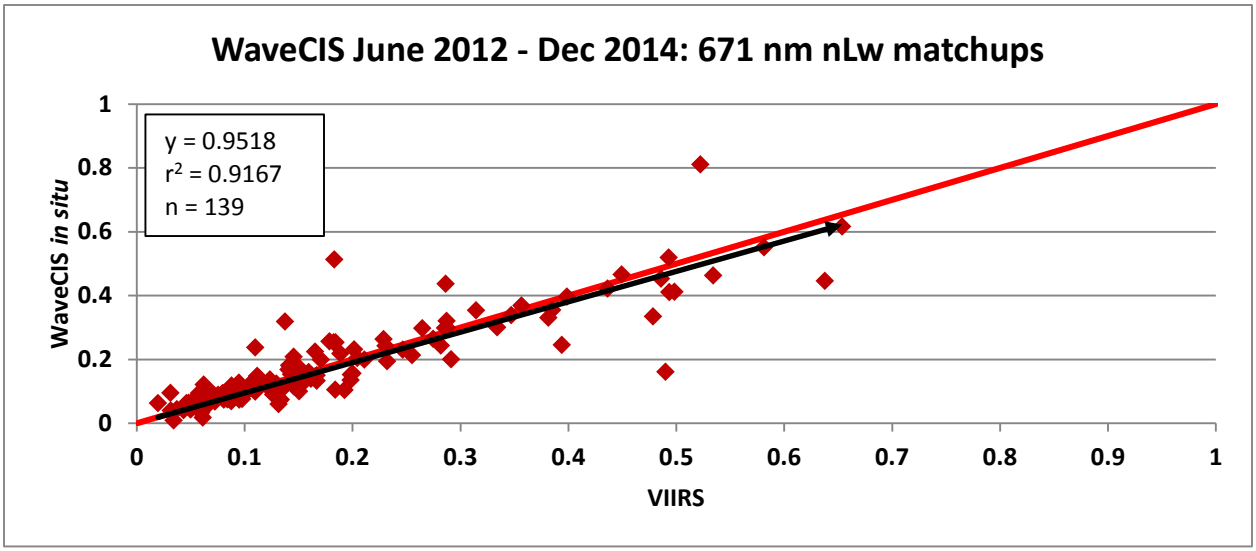

Figure 20 shows the 671 nm (M5) nLw matchups between the satellite and *in situ* data from the WaveCIS site from 1 Jun 2012 up to 31 Dec 2014. Matchups are minimally screened, removing: negative values at any wavelength, extreme viewing angles, glint, clouds, navigation failures, atmospheric failures. A red 1:1 line is provided for reference. The regression and correlation coefficients indicate a tight correlation (close to 1) between the satellite and *in situ* sensors. Notice the range of VIIRS (0.02 – 0.62) more appropriately covers the natural range of nLw seen in open ocean and coastal waters, *compare to MOBY (0.01, 0.05)*. Also, note the higher correlation coefficient as compared to the same channel at MOBY (where r^2 = 0.6588). This is due to stronger signal to noise and sensitivity of this channel in the coastal waters.

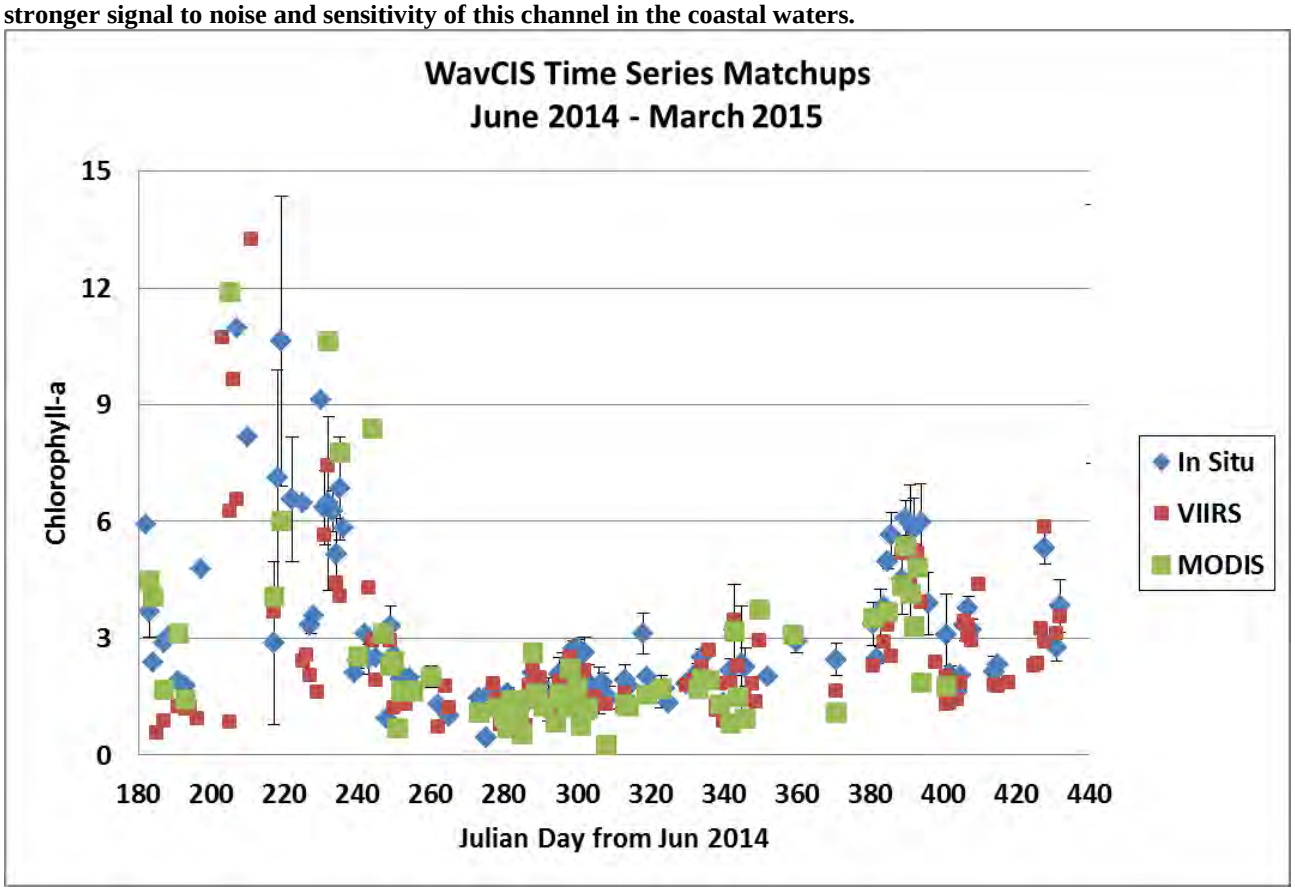

Figure 21 provides the time series of the Level 3 chlorophyll products where the daily mean of *in situ* is shown in blue, the VIIRS center pixel is red, and MODIS center pixel is green. To help understand the daily time variance of chlorophyll values in the coastal ocean, the error bars show the standard deviation around the *in situ* daily mean.

Both satellites adequately track the trend at the ground truth station. ***Note both sensors' vicarious calibrations were updated and both sensors are consistent -- agreeing well.***

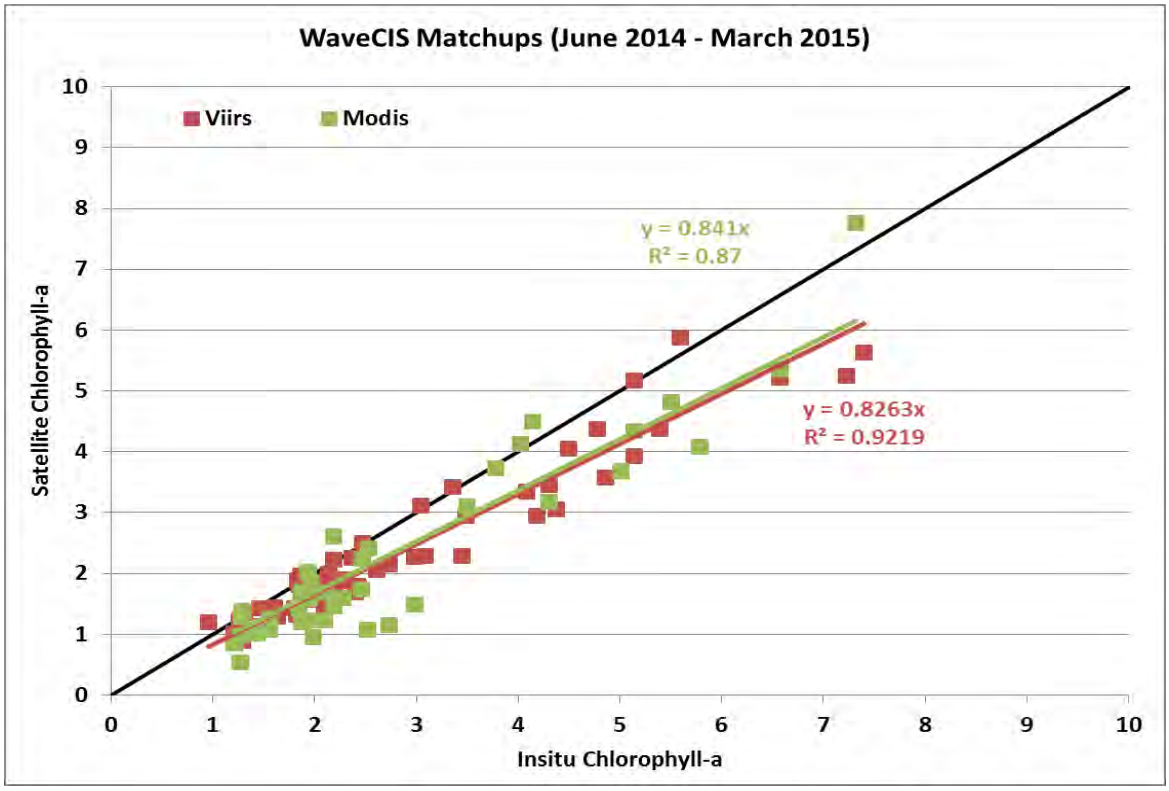

Figure 22 shows the regression analysis of the VIIRS and MODIS Level 3 chlorophyll products to the WaveCIS *in situ* derived chlorophyll. VIIRS and MODIS provide comparable results. The correlation of VIIRS is slightly stronger than the MODIS:*in situ* relationship.

3.3.2.2 Yellow Sea – GOCI, VIIRS and MODIS

To evaluate the current AOPS v4.12 processing of GOCI level 1b water leaving radiance (nL_w), we provide an inter-sensor comparison between GOCI, MODIS, and VIIRS products. This comparison was performed in the Yellow Sea with limited AERONET-OC from the IEODO station. Unfortunately, a significant number of *in situ* matchups were not available as the IEODO system has not yet reached the maturity level of other AERONET-OC locations[6]. *Due to the lack of in situ data in this region, the vicarious calibration of GOCI was performed using MODIS as synthetic in situ data at the site. These are the vicarious calibration gains implemented in AOPS v4.12 (ref. Table 3).*

Figure 23 shows the GOCI, VIIRS and MODIS beam attenuation products in the Yellow Sea, October 28, 2014. The MODIS data, processed with appropriate calibration coefficients, represents truth (top center). The top left and right panels show the GOCI and VIIRS processed without vicarious calibration coefficients. The unity calibration for both sensors provides higher retrievals than the same day MODIS

[6] There were 16 (level 1.5) measurements at Ieodo available for download in calendar year 2014.

image. Bottom left and right images were created with AOPS v4.12 by applying the individual sensor gains from the corresponding tables in section 2. Both sensors show improved performance as compared to MODIS.

Figure 24 shows the GOCI (bottom row), VIIRS (center row) and MODIS (top row) vertical visibility products in the Yellow Sea, October 28, 2014 for unity/ AOPS beta version (left column), AOPS v4.10 (center column) and AOPS v4.12 (right column). The MODIS data processed with appropriate calibration coefficients using AOPS v4.12 represents truth (top right). Notice that the top row (MODIS) for all three gain sets / versions shows that the MODIS calibration is stable. The left column (unity gains – *i.e. no vicarious calibration*) indicates poor agreement between all three sensors. The center column processed with AOPS v4.10 shows improvement for VIIRS and GOCI compared to MODIS. The right column processed with AOPS v4.12 shows a major improvement for VIIRS and GOCI for the Navy vertical visibility product and indicates all three sensors are consistent, showing reasonable agreement.

Figure 25 shows the GOCI, VIIRS and MODIS chlorophyll products at the IEODO station in the Yellow Sea, March 16, 2014. The top left and right panels show the MODIS and VIIRS chlorophyll products. The GOCI chlorophyll image is shown in the bottom left. The bottom right panel shows the spectral remote sensing reflectance comparisons for the same day at the IEODO *in situ* AERONET-OC station (blue) and corresponding pixels from MODIS (red), VIIRS (green) and GOCI (orange). Defining the *in situ* point as truth, all three sensors capture the spectral signature at the location. Additional IEODO/*in situ* data is needed to define the accuracy and uncertainty of the retrievals.

Figure 26 to Figure 28 show the comparison of several derived products derived from the MODIS, VIIRS and GOCI sensors. In each case the trend is expressed by all three sensors although variation in the absolute magnitude indicates additional work on some combination of calibration and algorithm development could improve the results.

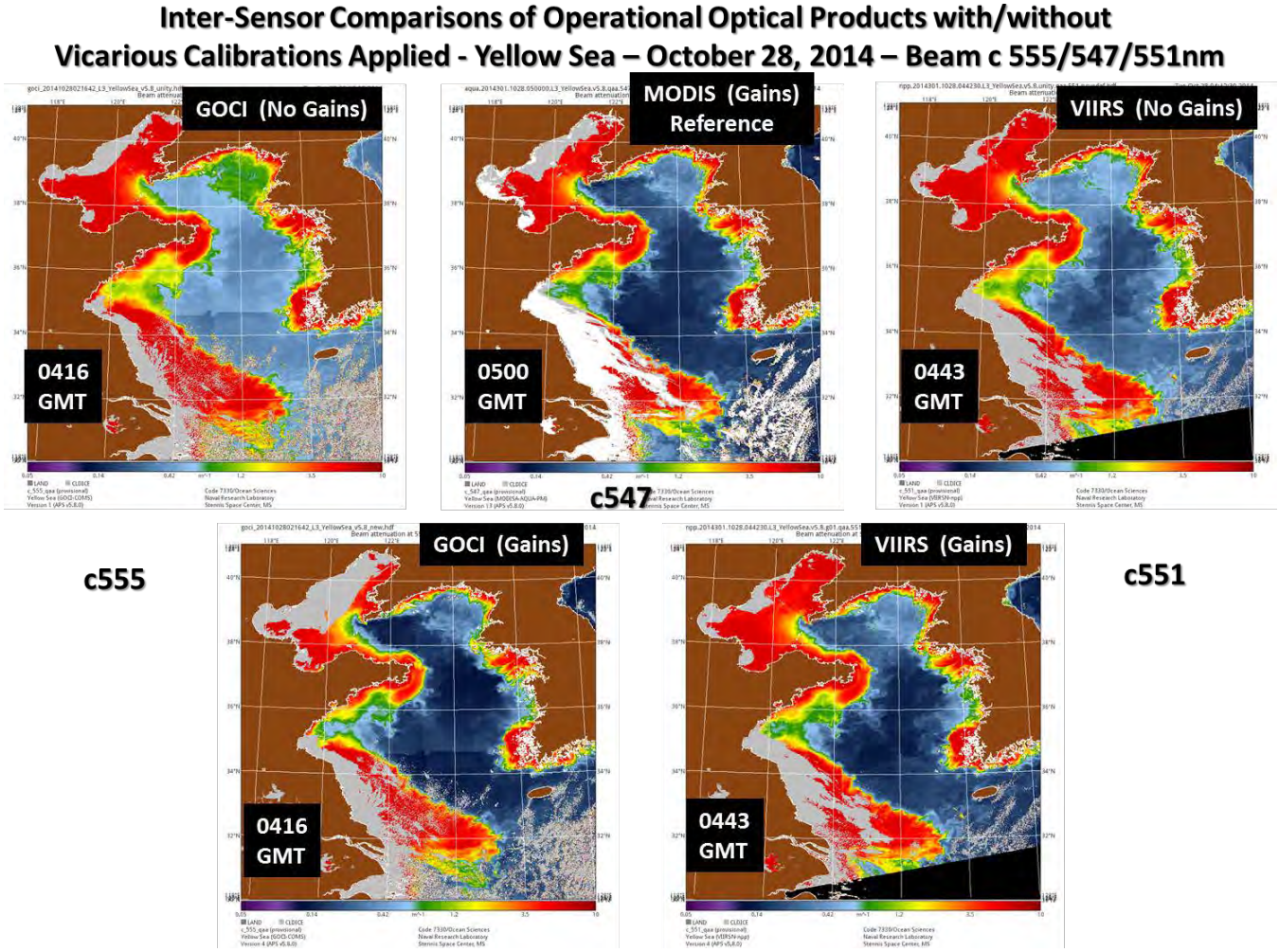

Figure 23 shows the GOCI, VIIRS and MODIS beam attenuation products in the Yellow Sea, October 28, 2014. The MODIS data, processed with appropriate calibration coefficients, represents truth (top center). The top left and right panels show the GOCI and VIIRS processed without vicarious calibration coefficients. The unity calibration for both sensors provides higher retrievals than the same day MODIS image. Bottom left and right images were created with AOPS v4.12 by applying the individual sensor gains from the corresponding tables in section 2. Both sensors show improved performance as compared to MODIS.

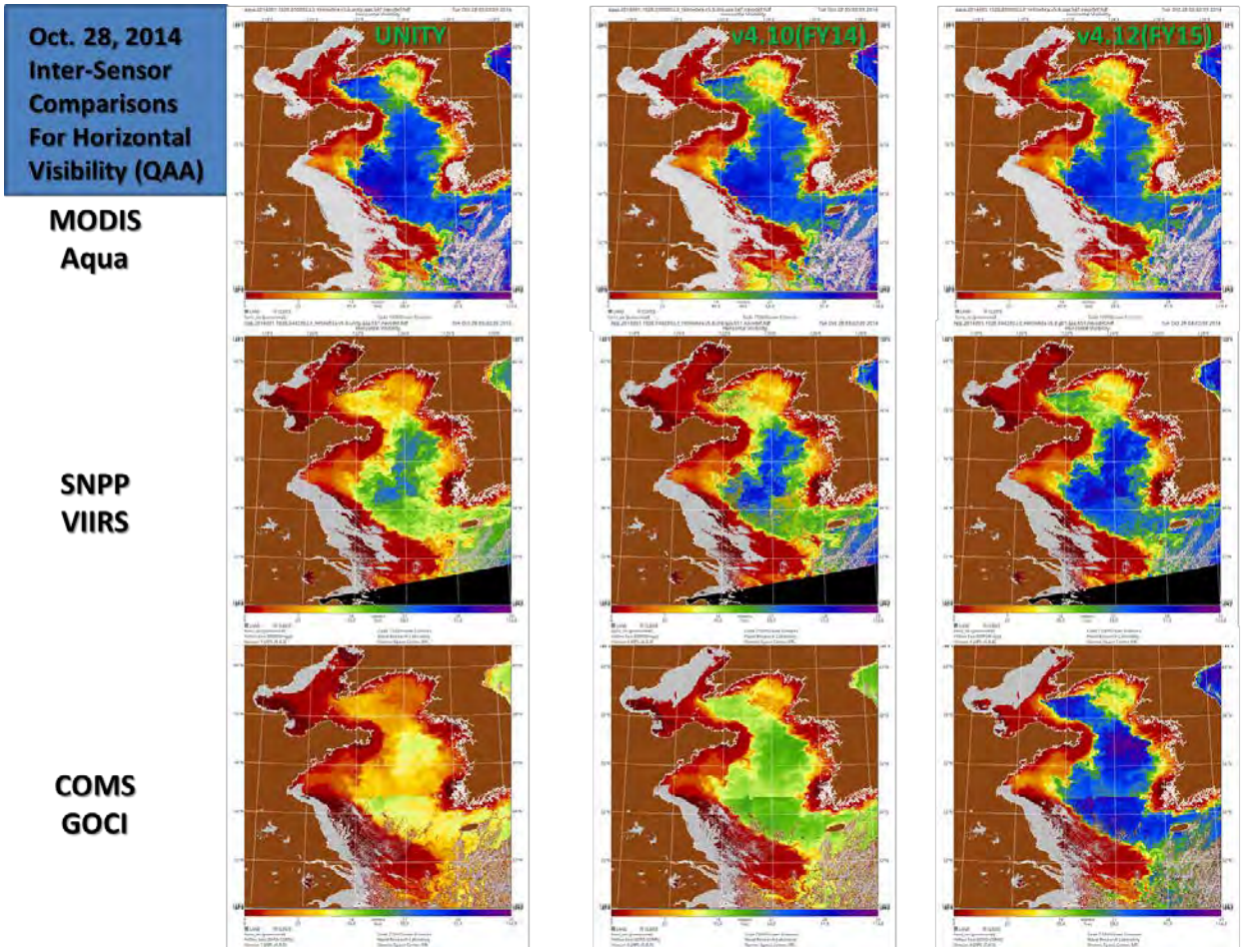

Figure 24 shows the GOCI (bottom row), VIIRS (center row) and MODIS (top row) vertical visibility products in the Yellow Sea, October 28, 2014 for unity/ AOPS beta version (left column), AOPS v4.10 (center column) and AOPS v4.12 (right column). The MODIS data processed with appropriate calibration coefficients using AOPS v4.12 represents truth (top right). Notice that the top row (MODIS) for all three gain sets / versions shows that the MODIS calibration is stable. The left column (unity gains – *i.e. no vicarious calibration*) indicates poor agreement between all three sensors. The center column processed with AOPS v4.10 shows improvement for VIIRS and GOCI compared to MODIS. The right column processed with AOPS v4.12 shows a major improvement for VIIRS and GOCI for the Navy vertical visibility product and indicates all three sensors are consistent, showing reasonable agreement.

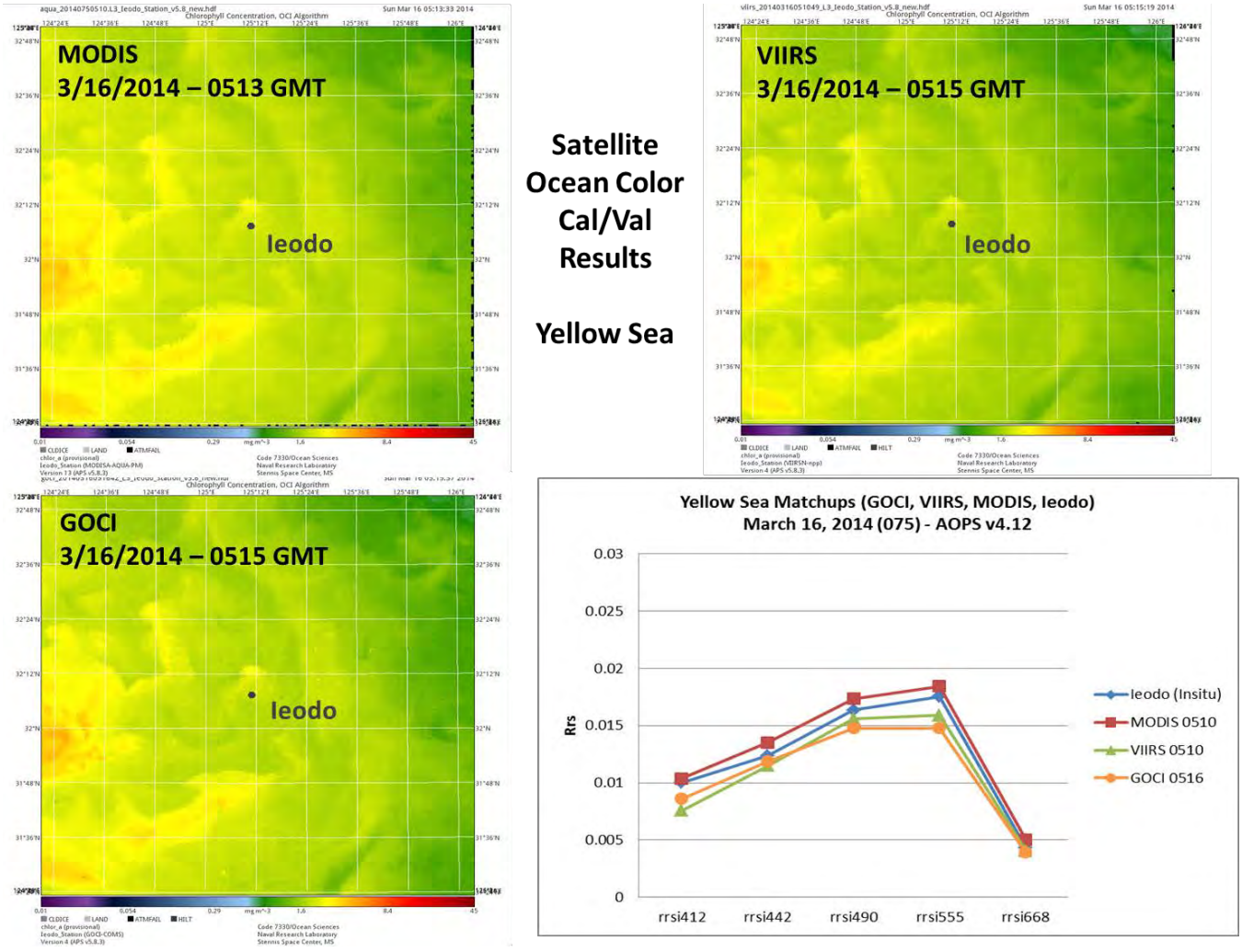

Figure 25 shows the GOCI, VIIRS and MODIS chlorophyll products at the IEODO station in the Yellow Sea, March 16, 2014. The top left and right panels show the MODIS and VIIRS chlorophyll products. The GOCI chlorophyll image is shown in the bottom left. The bottom right panel shows the spectral remote sensing reflectance comparisons for the same day at the IEODO *in situ* AERONET-OC station (blue) and corresponding pixels from MODIS (red), VIIRS (green) and GOCI (orange). Defining the *in situ* point as truth, all three sensors capture the spectral signature at the location. Additional IEODO/*in situ* data is needed to define the accuracy and uncertainty of the retrievals.

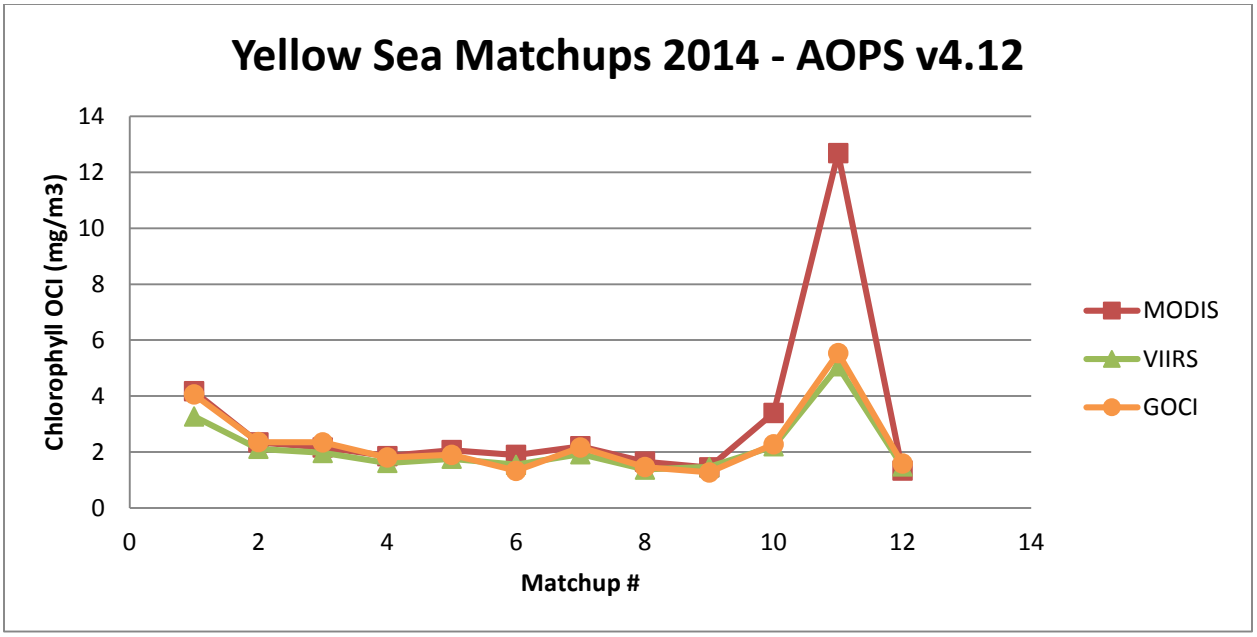

Figure 26 shows the chlorophyll products from GOCI with the same day MODIS and VIIRS chlorophyll retrievals, where n = 12, representing quality scenes for all three sensors throughout 2014. The GOCI retrievals are reasonable in comparison to VIIRS and MODIS. The eleventh matchup suggests there was an anomaly with the MODIS reading for that day *likely due to the pixel being inappropriately flagged/masked*, as it is not also expressed in either the VIIRS or GOCI sensors.

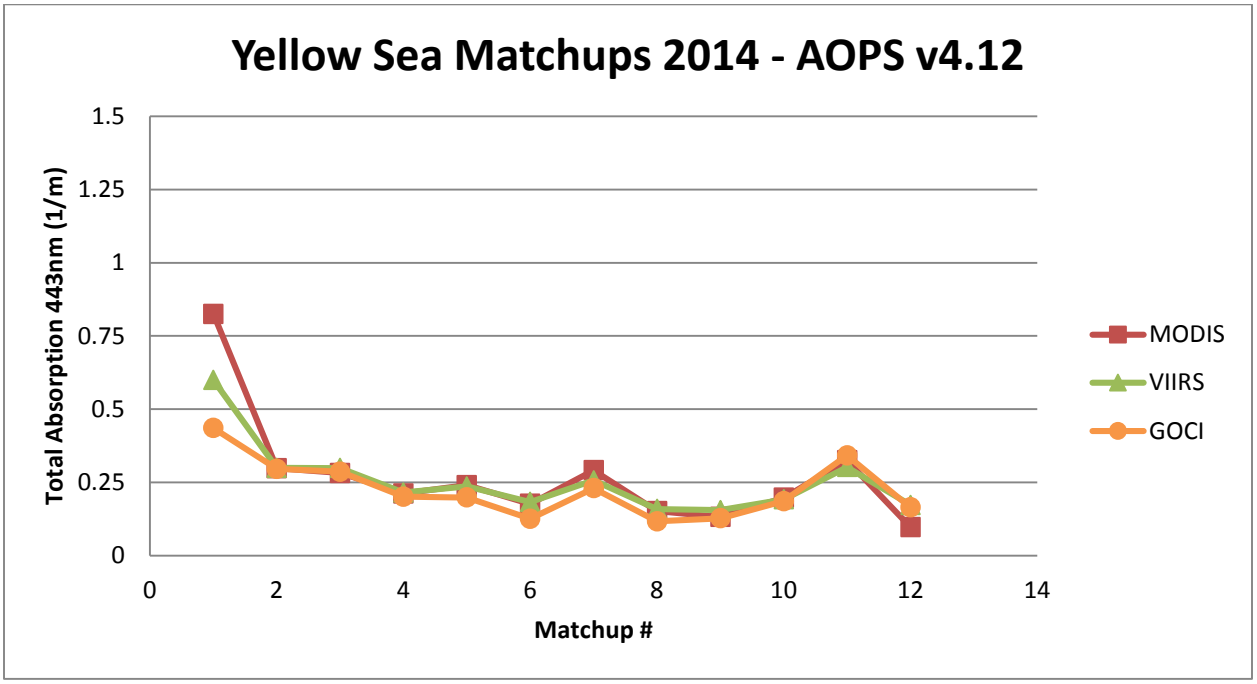

Figure 27 shows the total absorption products from GOCI with the same day MODIS and VIIRS retrievals, where n = 12, representing quality scenes for all three sensors throughout 2014. The GOCI retrievals are reasonable in comparison to VIIRS and MODIS. The first matchup shows some differences but in a spatially and temporally dynamic system is not unexpected. Notice the 443 nm at sample eleven is reasonable suggesting the 488 of MODIS may have been the issue for OCI chlorophyll retrieval in the previous figure.

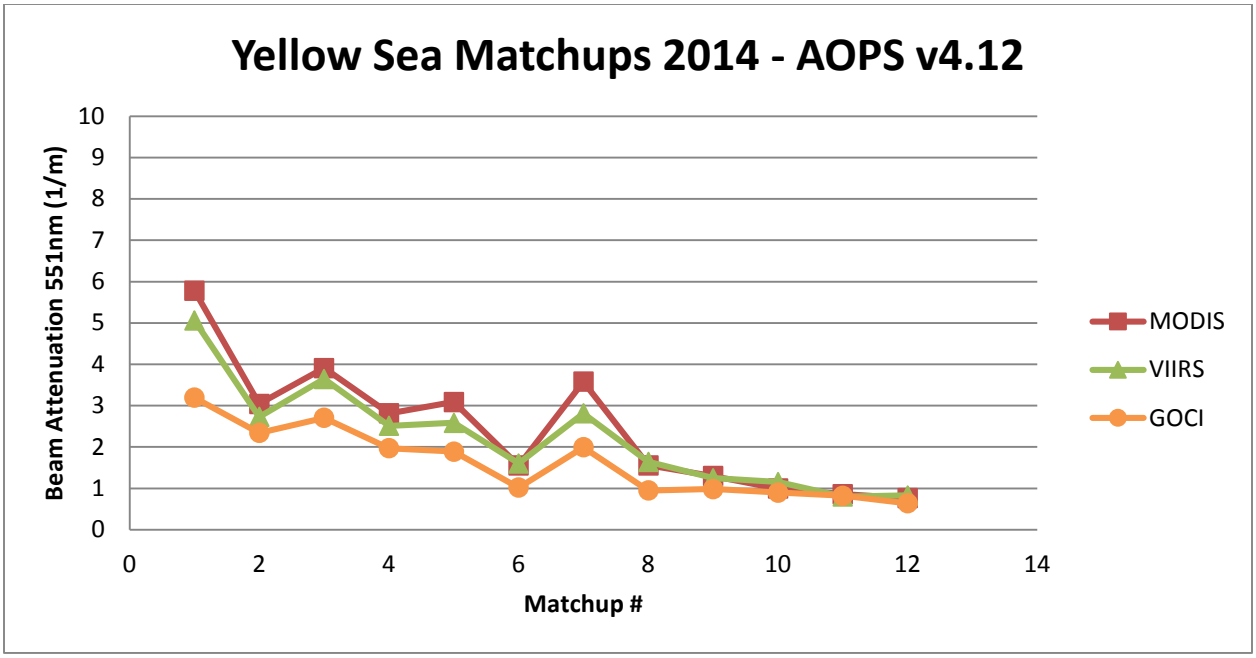

Figure 28 shows the beam attenuation coefficients from GOCI with the same day MODIS and VIIRS retrievals, where n = 12, representing quality scenes for all three sensors throughout 2014. The GOCI retrievals are low in comparison to VIIRS and MODIS but follow a similar trend. The first and seventh matchups show some differences but in a spatially and temporally dynamic system these differences are not unexpected. Also the beam attenuation is a derived product therefore any discrepancies reflect the limitations of the algorithms (bb to b conversion, etc.) in addition to being an indicator of satellite performance. Taken as a whole, these products indicate additional data collection and work on calibration and algorithm development for the GOCI would improve the products.

3.3.2.3 Cruise data

As part of the NOAA Cal/Val effort, validation data was collected during the GEOCAPE cruise off the Gulf of Mexico in September of 2013. Data was collected by the University of Massachusetts, Boston. The following figures provide an assessment of the performance of VIIRS Rrs retrievals against the *in situ* measurement. The corresponding MODIS comparison is also provided as a baseline. For a variety of environmental reasons, the satellite to *in situ* relationships should improve with longer wavelengths in coastal waters.

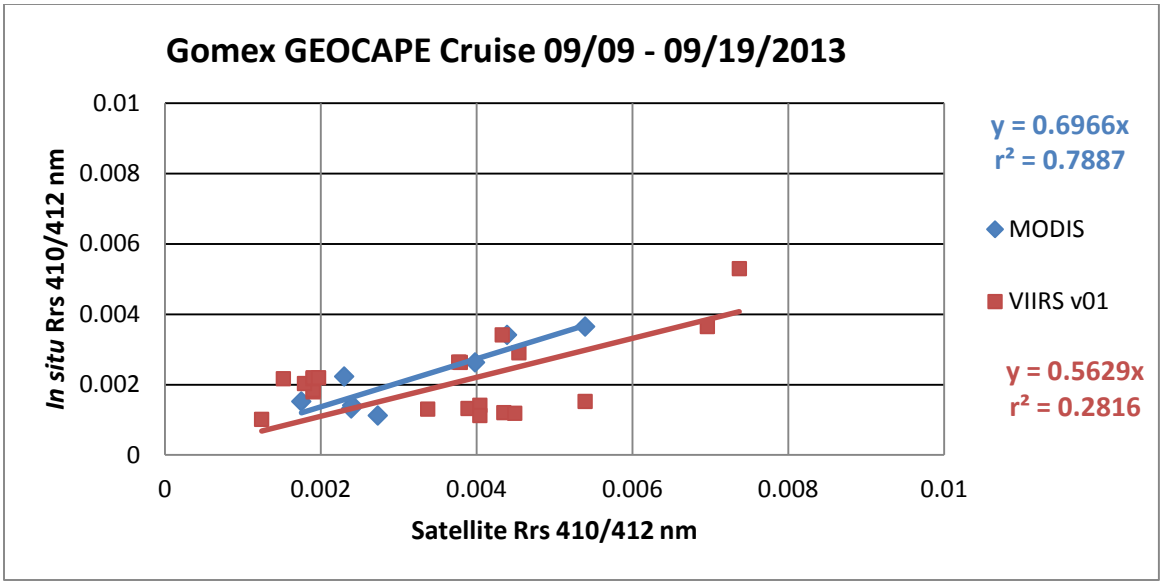

Figure 29 shows the VIIRS 410 nm and MODIS 412 nm Rrs matchups between the satellite and *in situ* data from the GEOCAPE cruise, September 2013. MODIS data is shown in blue and VIIRS in red. At this wavelength, MODIS shows a reasonable correlation between the satellite and *in situ* sensors; however VIIRS retrievals show a 0.56 slope and low correlation coefficient. Both satellite techniques produce results that are too high as compared to the *in situ* measurement. Discrepancies could be due to a combination of factors including instrumentation differences, complex marine atmospheric conditions close to the coast and very likely the dynamic spatial and temporal changes in the in water constituents (particles, dissolved organic material, phytoplankton).

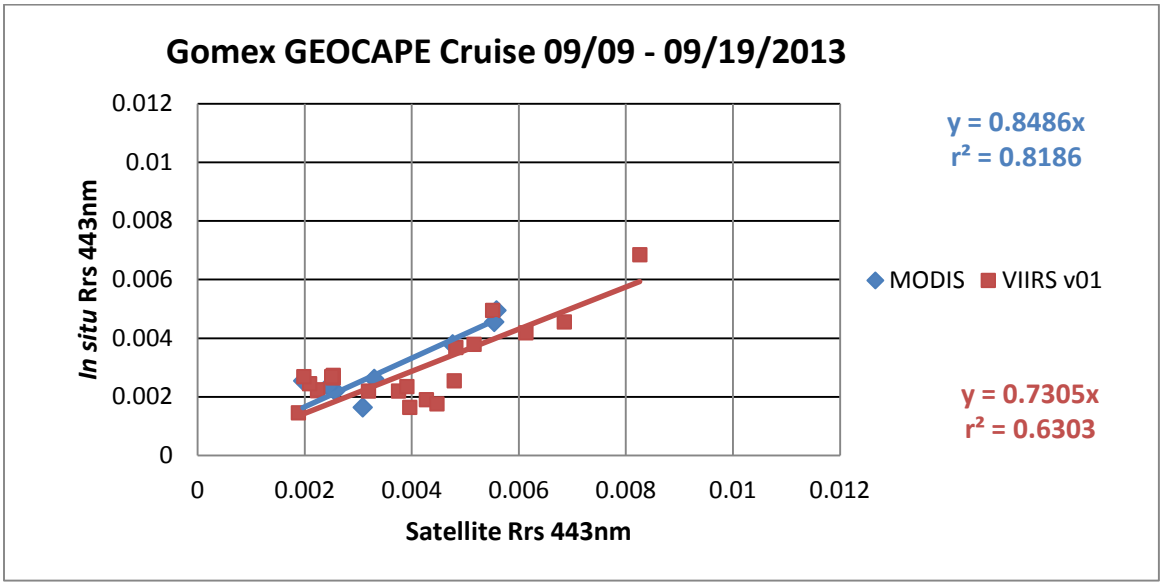

Figure 30 shows the 443 nm Rrs matchups between the satellite and *in situ* data from the GEOCAPE cruise, September 2013. MODIS data is shown in blue and VIIRS in red. At this wavelength, MODIS and VIIRS show a reasonable correlation between the satellite and *in situ* sensors. Both satellite retrievals produce results that are too high. Discrepancies could be due to a combination of factors including instrumentation differences, complex marine atmospheric conditions close to the coast and very likely the dynamic spatial and temporal changes in the in water constituents (particles, dissolved organic material, phytoplankton).

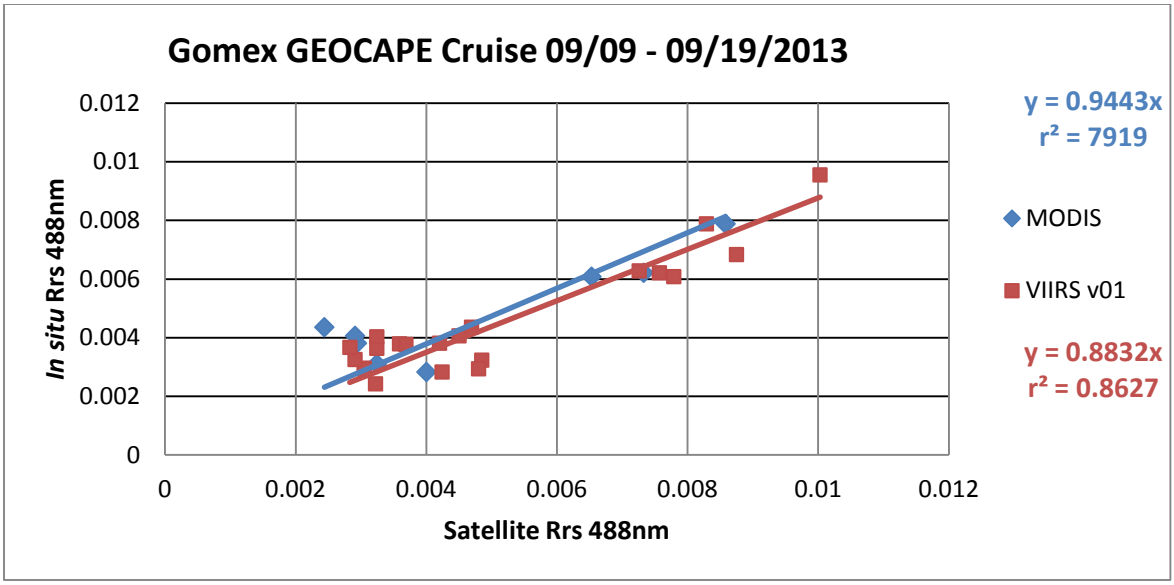

Figure 31 shows the 488 nm Rrs matchups between the satellite and *in situ* data from the GEOCAPE cruise, September 2013. MODIS data is shown in blue and VIIRS in red. At this wavelength, MODIS and VIIRS show a good correlation between the satellite and *in situ* sensors. The VIIRS satellite retrievals are a little high. Discrepancies could be due to a combination of factors including instrumentation differences, complex marine atmospheric conditions close to the coast and the dynamic spatial and temporal changes in the in water constituents (particles, dissolved organic material, phytoplankton).

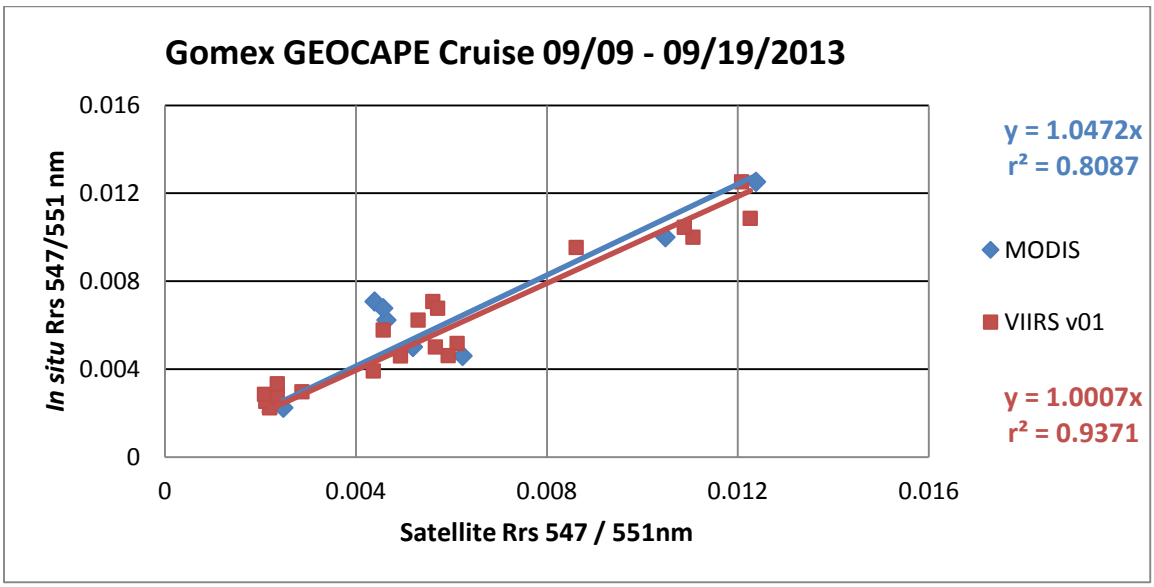

Figure 32 shows the MODIS 547 nm and VIIRS 551 nm Rrs matchups between the satellite and *in situ* data from the GEOCAPE cruise, September 2013. MODIS data is shown in blue and VIIRS in red. At this wavelength, MODIS and VIIRS show very good correlation between the satellite and *in situ* sensors.

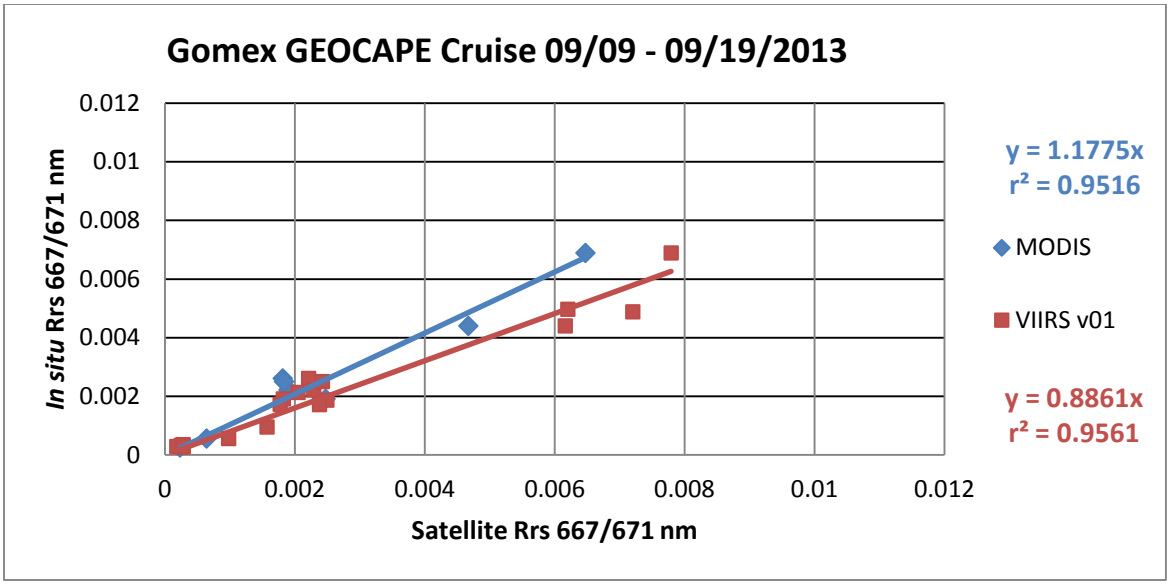

Figure 33 shows the MODIS 667 nm and VIIRS 671 nm Rrs matchups between the satellite and *in situ* data from the GEOCAPE cruise, September 2013. MODIS data is shown in blue and VIIRS in red. At this wavelength, MODIS and VIIRS show a good correlation between the satellite and *in situ* sensors. The MODIS satellite retrievals are a little low and VIIRS satellite retrievals are a little high. Discrepancies could be due to several factors including instrumentation differences, complex marine atmospheric conditions close to the coast and the dynamic spatial and temporal changes in the in water constituents (particles, dissolved organic material, phytoplankton).

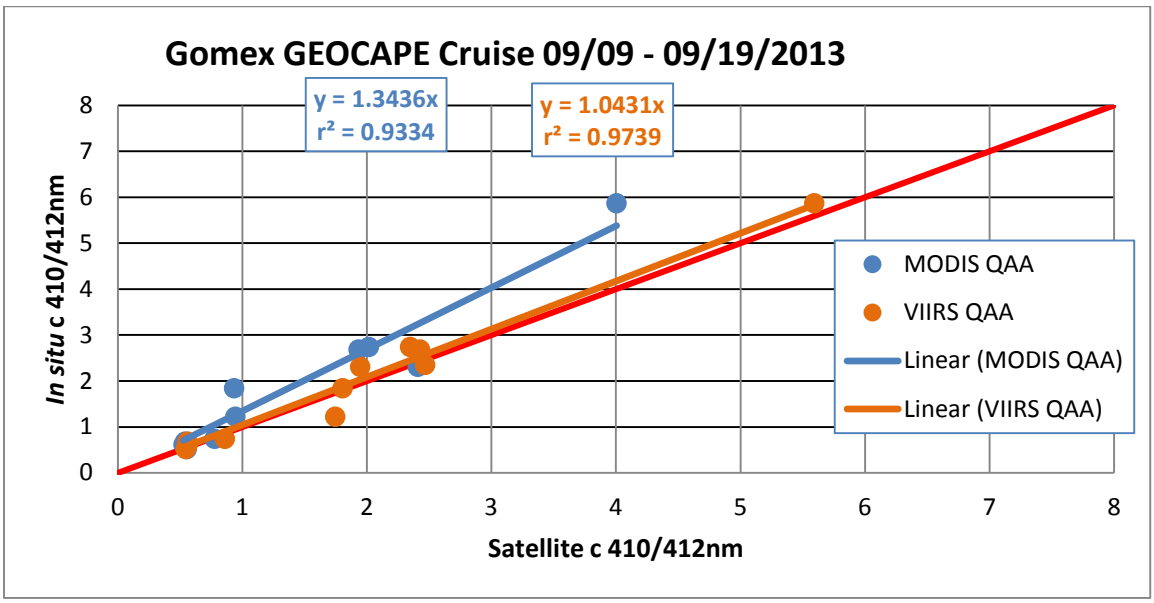

Figure 34 shows the VIIRS 410 nm and MODIS 412 nm QAA derived beam attenuation (c) matchups between the satellite and *in situ* data from the GEOCAPE cruise, September 2013. MODIS data is shown in blue and VIIRS in orange. At this wavelength, MODIS shows a strong linear relationship (r^2) and VIIRS show a better correlation between the satellite and *in situ* sensor. The MODIS satellite retrievals are a little low. Discrepancies could be due to several factors including instrumentation differences, complex marine atmospheric conditions close to the coast and the dynamic spatial and temporal changes in the in water constituents (particles, dissolved organic material, phytoplankton) and algorithm sensitivities.

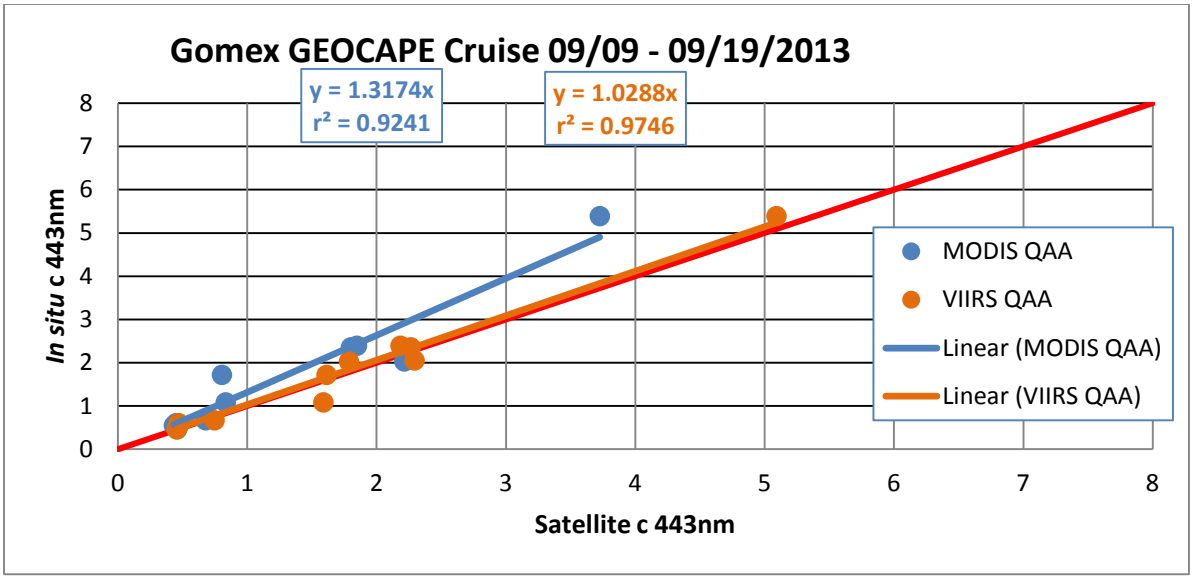

Figure 35 shows the 443 nm QAA derived beam attenuation matchups between the satellite and *in situ* data from the GEOCAPE cruise, September 2013. MODIS data is shown in blue and VIIRS in orange. At this wavelength, MODIS shows a strong linear relationship (r^2) and VIIRS show a better correlation between the satellite and *in situ* sensor. The MODIS satellite retrievals are a little low. Discrepancies could be due to several factors including instrumentation differences, complex marine atmospheric conditions close to the coast and the dynamic spatial and temporal changes in the in water constituents (particles, dissolved organic material, phytoplankton) and algorithm sensitivities.

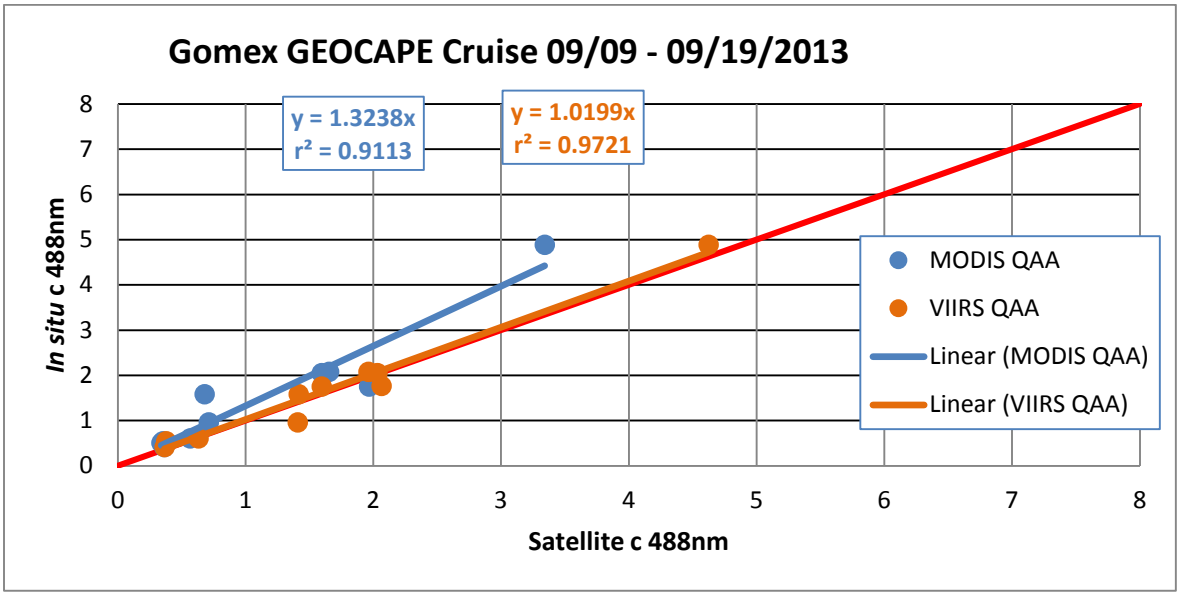

Figure 36 shows the 488 nm QAA derived beam attenuation matchups between the satellite and *in situ* data from the GEOCAPE cruise, September 2013. MODIS data is shown in blue and VIIRS in orange. At this wavelength, MODIS shows a strong linear relationship (r^2) and VIIRS show a better correlation between the satellite and *in situ* sensor. The MODIS satellite retrievals are a little low. Discrepancies could be due to several factors including instrumentation differences, complex marine atmospheric conditions close to the coast and the dynamic spatial and temporal changes in the in water constituents (particles, dissolved organic material, phytoplankton) and algorithm sensitivities.

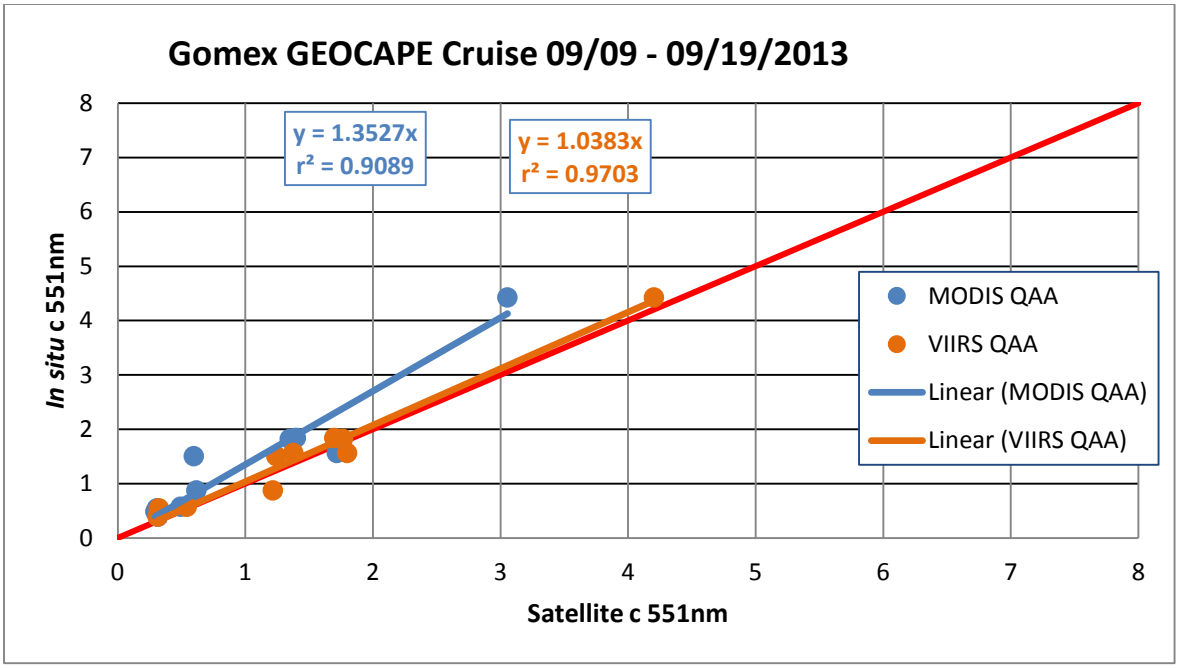

Figure 37 shows the 551 nm QAA derived beam attenuation matchups between the satellite and *in situ* data from the GEOCAPE cruise, September 2013. MODIS data is shown in blue and VIIRS in orange. At this wavelength, MODIS shows a strong linear relationship (r^2) and VIIRS show a better correlation between the satellite and *in situ* sensor. The MODIS satellite retrievals are a little low. Discrepancies could be due to several factors including instrumentation differences, complex marine atmospheric conditions close to the coast and the dynamic spatial and temporal changes in the in water constituents (particles, dissolved organic material, phytoplankton) and algorithm sensitivities.

3.4 High Resolution VIIRS

The spatial dynamics of coastal and inland regions are highly variable and require the use of increased spatial resolution monitoring from ocean color remote sensors. A procedure for the spatial enhancement of VIIRS ocean color products, including derivation of chlorophyll and IOPs, was developed using a sharpened visible water-leaving radiance spectrum. This new approach utilizes the spatial covariance of the spectral bands for sharpening the M bands (412, 443, 486, 551, 671 nm; 750-m resolution) with the I-1 band (645 nm; 375-m resolution). The spectral shape remains consistent by the use of a dynamic, wavelength-specific spatial resolution ratio that is weighted as a function of the relationship between proximate I- and M-band variance at each pixel. A comparison of bio-optical satellite products at 375-m and 750-m spatial resolution with *in situ* measurements of water leaving radiance and bio-optical properties show an improved capability of the VIIRS 375-m products in turbid and optically complex waters such as the Chesapeake Bay and Mississippi River Plume. We demonstrate that the increased spatial resolution improves the ability for VIIRS to characterize bio-optical properties in coastal waters (Vandermeulen et al., *In Press, RSE*).

Qualitative results show increased resolution for the visible nLw spectrum with no significant change to the spectral shape, yielding enhanced feature detection compared to M(λ) 750-m products. These 375-m radiance products are re-processed to calculate bio-optical SNPP-VIIRS products at 375-m spatial resolution. The sharpened products show no spectral artifacts, such as speckling, or any extreme changes

in the relative magnitude of derived values. Quantitative matchups of VIIRS data with a diverse collection of *in situ* radiance values and geophysical parameters show that the VIIRS 375-m data set 1) does not express sensitivity to band ratio or semi-analytical algorithms and 2) significantly increases the quality of returns for the full nLw spectrum and QAA products in comparison to the 750-m dataset. Large improvements to feature detection are also quantified and validated with a flow through dataset, demonstrating that the 375-m bio-optical products yield information that cannot be resolved at 750-m spatial resolution.

Figure 38 provides a multi-regional comparison of VIIRS backscattering product at 551 nm using the QAA algorithm. Left most vertical panel gives the areas of interest: (top) Mississippi River Plume on May 14, 2013, (middle) Chesapeake Bay on April 6, 2013 and 9 bottom) San Francisco Bay on January 16, 2013. The center vertical series shows the standard 750 m resolution product for each area and the right vertical series shows the 375 m resolution enhanced product using the weighted ratio sharpening technique. Small errors in the spectral sharpening technique have the potential to be propagated and enhanced when pushed through the QAA. The absence of visual irregularities and qualitative improvement of frontal features demonstrate the advantages of band-sharpening in coastal and inland waters.

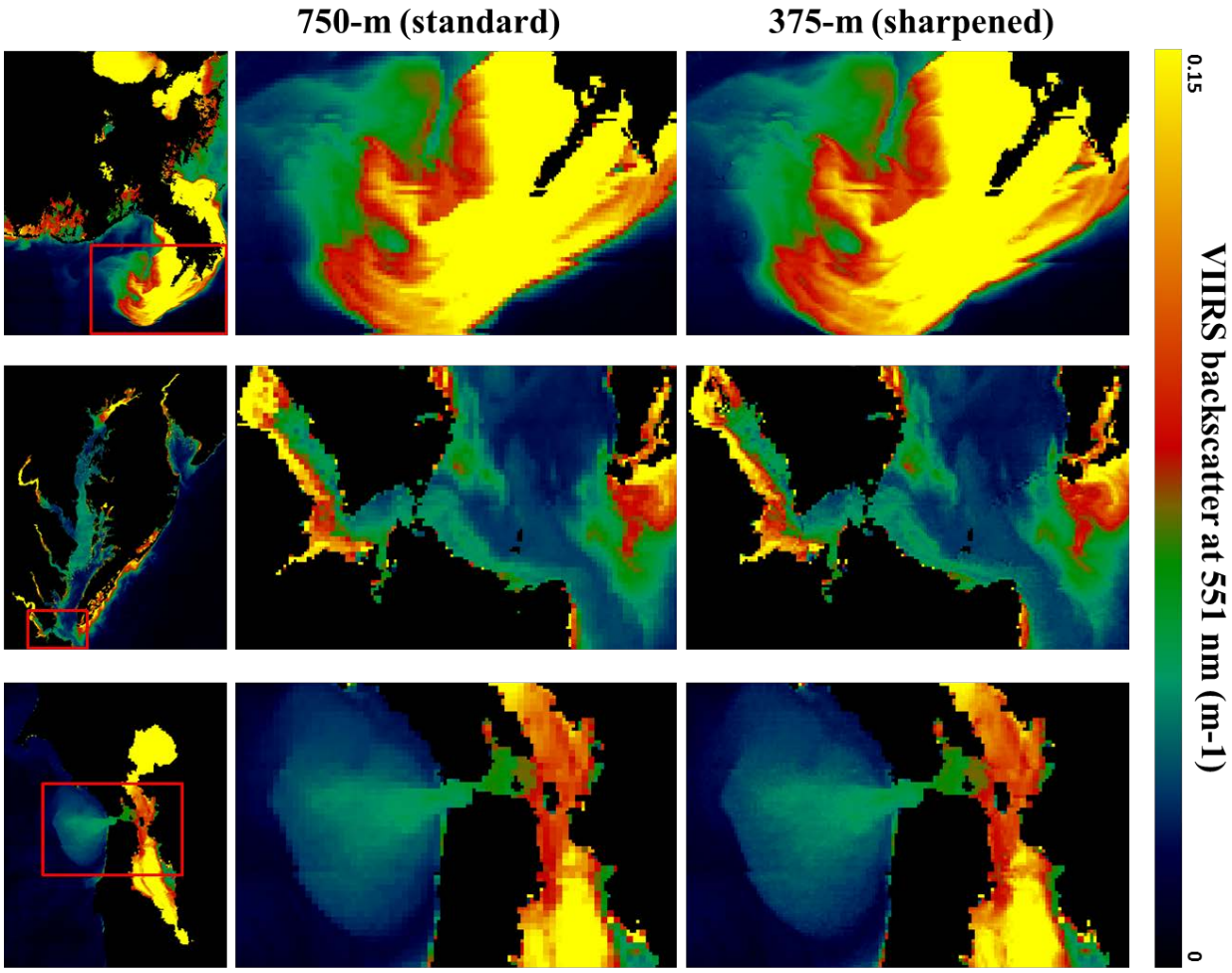

Figure 38 provides a multi-regional comparison of VIIRS backscattering product at 551 nm using the QAA algorithm. Left most vertical panel gives the areas of interest: (top) Mississippi River Plume on May 14, 2013, (middle) Chesapeake Bay on April 6, 2013 and 9 bottom) San Francisco Bay on January 16, 2013. The center vertical series shows the standard 750 m resolution product for each area and the right vertical series shows the 375 m resolution enhanced product using the weighted ratio sharpening technique. Small errors in the spectral sharpening technique have the potential to be propagated and enhanced when pushed through the QAA. The absence of visual irregularities and qualitative improvement of frontal features demonstrate the advantages of band-sharpening in coastal and inland waters.

The quality of the sharpening algorithm was evaluated by analyzing satellite to *in situ* matchups of water leaving radiance. Figure 39 shows a scatter plot of the VIIRS^{375m} and VIIRS^{750m} center pixel nLw retrievals for all wavelengths against a diverse collection of *in situ* spectral matchups. The data show an overall higher R value for the comparison between the *in situ* data and the VIIRS^{375m} dataset, relative to the VIIRS^{750m} dataset. This suggests reasonable capability of the sharpened satellite data to represent *in situ* data and demonstrates there are no major outliers introduced by the sharpening algorithm.

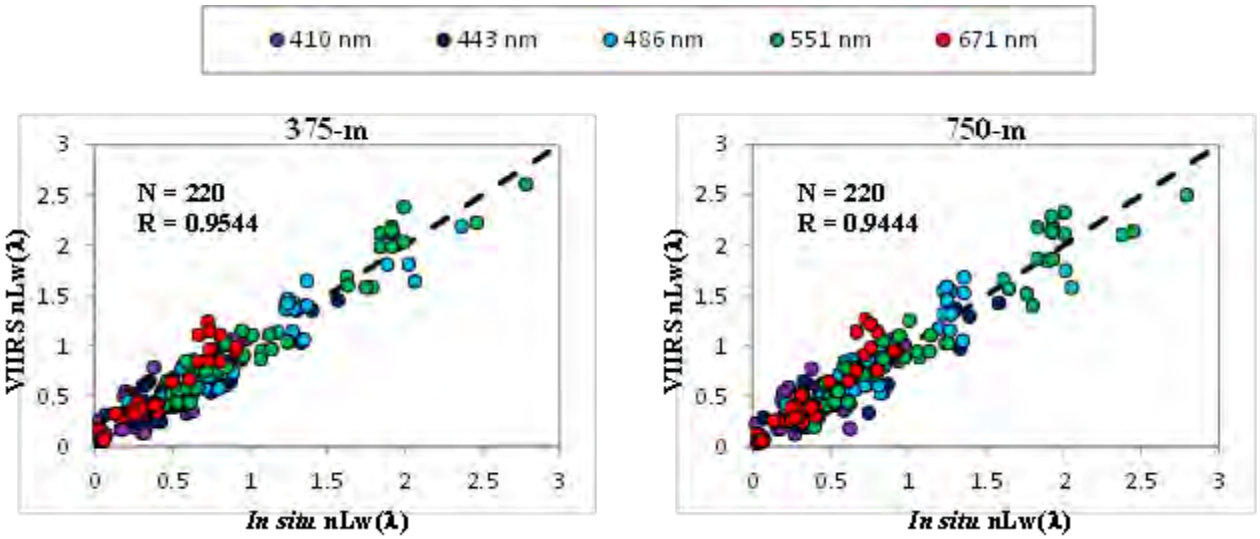

Figure 39 shows a scatter plot of normalized water leaving radiance (mW/cm2/m/sr), comparing the 220 in situ data points in various types to the corresponding single pixel VIIRS extraction at 375-m resolution (Left) and 750-m resolution (Right). Note that no major outliers are introduced by the VIIRS 375-m series, suggesting that the VIIRS data is not adversely impacted by the weighted sharpening technique.

As a final assessment of the sharpening algorithm performance, the enhancement of bio-optical feature detection is evaluated by comparison of satellite data with a high spatial resolution optical data set[7]. Figure 40 shows an *in situ* flow through dataset of IOPs binned to 375-m and compared to VIIRS-derived IOPs at 375-m and 750-m resolution. The map (A) shows the location of the cruise track corresponding to the plots, below showing that the VIIRS 375-m absorption at 443 nm (B) and beam attenuation at 551 nm (C) dataset more accurately characterizes the coastal waters and frontal features than the VIIRS 750-m dataset. Close to the satellite overpass (insets b-1, b-2) indicate the relative changes in total absorption from the *in situ* data set are more accurately represented by the VIIRS^{375m} dataset than the VIIRS^{750m} dataset. In this case, small spatial variability detected by the *in situ* dataset and the VIIRS^{375m} dataset are not well-defined by VIIRS^{750m}, presumably because the spatial binning of a 750-m pixel averages over the sub-pixel variability present (Lee et al. 2012). Inset C shows the comparison of *in situ* total beam attenuation (c) at 551 nm with satellite derived beam attenuation (c_551_qaa), demonstrating that many strong bio-optical fronts (insets, c-1, c-2, c-3, c-4) are better resolved with the VIIRS375m dataset. Note that the *in situ* data on either end of the plot (8 km and 40 km) represents a time lag of 1.5 hours from when the satellite data was collected, and shows a slight misalignment of the satellite estimated frontal features. In total this figure highlights the importance of closely aligning the temporal scales of collected data with the satellite measurements, especially in dynamic coastal waters.

[7] A high frequency IOP dataset was retrieved from an underway flow through system connected to a Wetlabs AC-9, courtesy of the Naval Research Laboratory's R/V Ocean Color cruise on November 20, 2013, 32-km cruise track in the northern Gulf of Mexico.

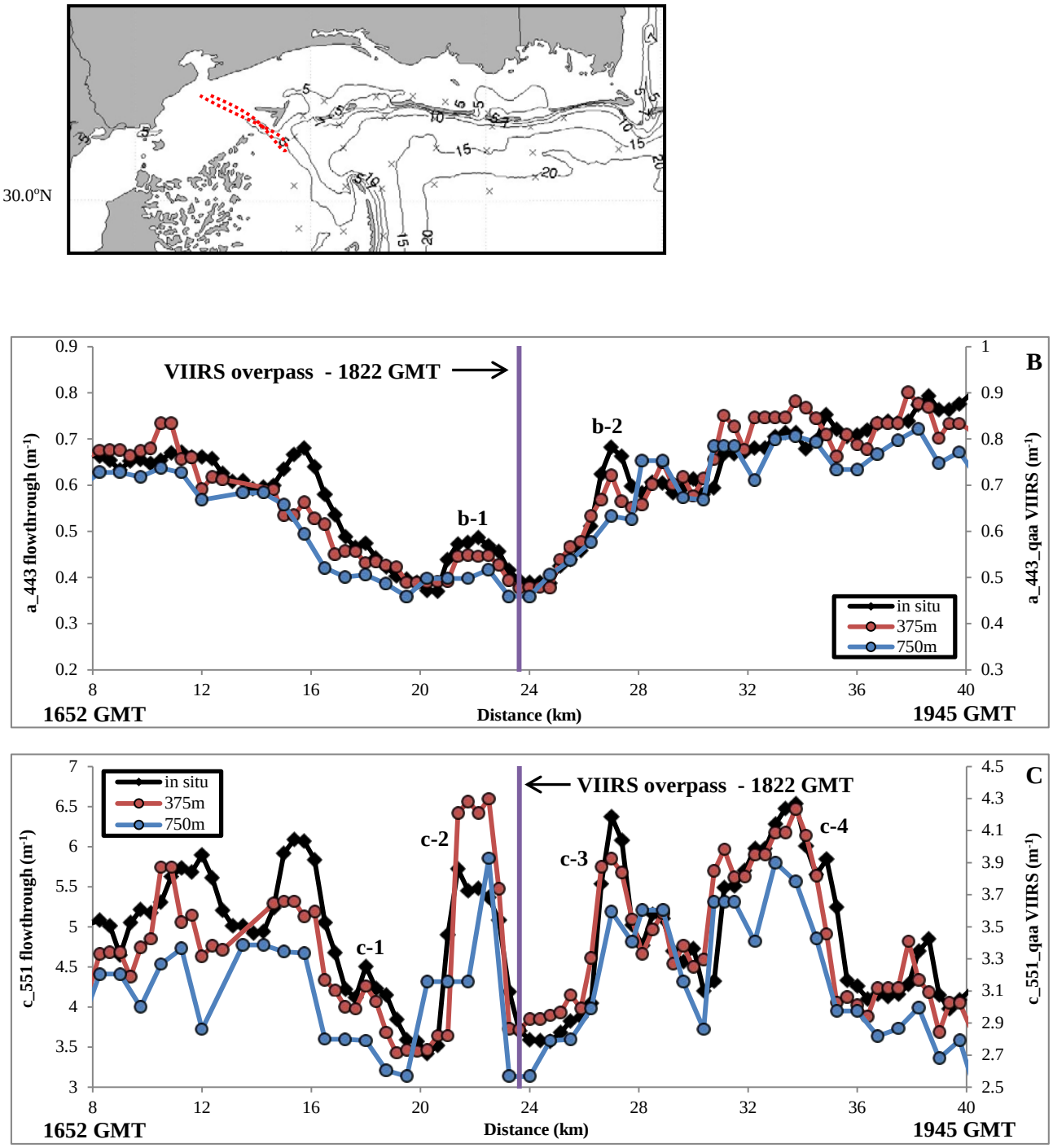

Figure 40 shows an in situ flow through dataset of IOPs binned to 375-m and compared to VIIRS-derived IOPs at 375-m and 750-m resolution. The map (A) shows the location of the cruise track corresponding to the plots, below showing that the VIIRS 375-m absorption at 443 nm (B) and beam attenuation at 551 nm (C) dataset more accurately characterizes the coastal waters and frontal features than the VIIRS 750-m dataset.

3.5 Algorithm update: Linear Matrix Inversion (LMI)

The LMI algorithm is a semi-analytical model. It is sophisticated in that the algorithm is a linear matrix requiring reflectance data from 3 wavelengths and 4 empirical parameters to describe the spectral shapes

of the individual IOP spectrum components *(a_phyto, a_dg, and bb_part),* (Hoge and Lyon, 1996). While the level of complexity makes LMI sensitive to a variety of spectral uncertainties, a noted strength is that it's regionally tunable, *where characteristics of in water constituents are constrained temporally and spatially,* given known or expected values.

Algorithm updates and improvements are necessary because the accuracy of retrievals of the IOPs (*output of LMI*) directly influences the accuracy of the required diver visibility products and other derived products, *such as LIDAR performance*. Figure 41 and Figure 42each show the before and after work on the LMI. The visibility product failures seen in Figure 41 were traced forward from calibration through the various levels of AOPS processing. The issue was ultimately resolved with regional tuning.

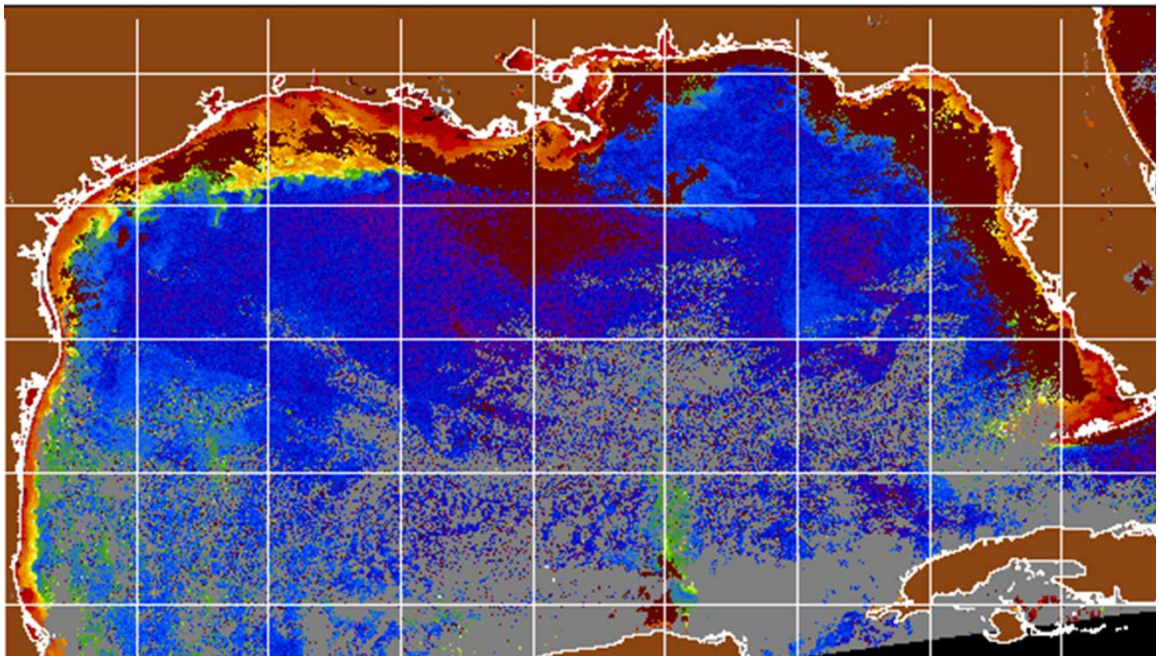

Figure 41 shows the horizontal visibility product from 25 Oct 2014 calculated using the VIIRS image and the LMI algorithm prior to adjustments. The maroon colored areas *(circled in red)* indicate algorithm failure. Algorithm failure can happen for a variety of reasons ranging from sensor calibration to variability in atmospheric and water composition, as well as unexpected variation in any of the algorithm components.

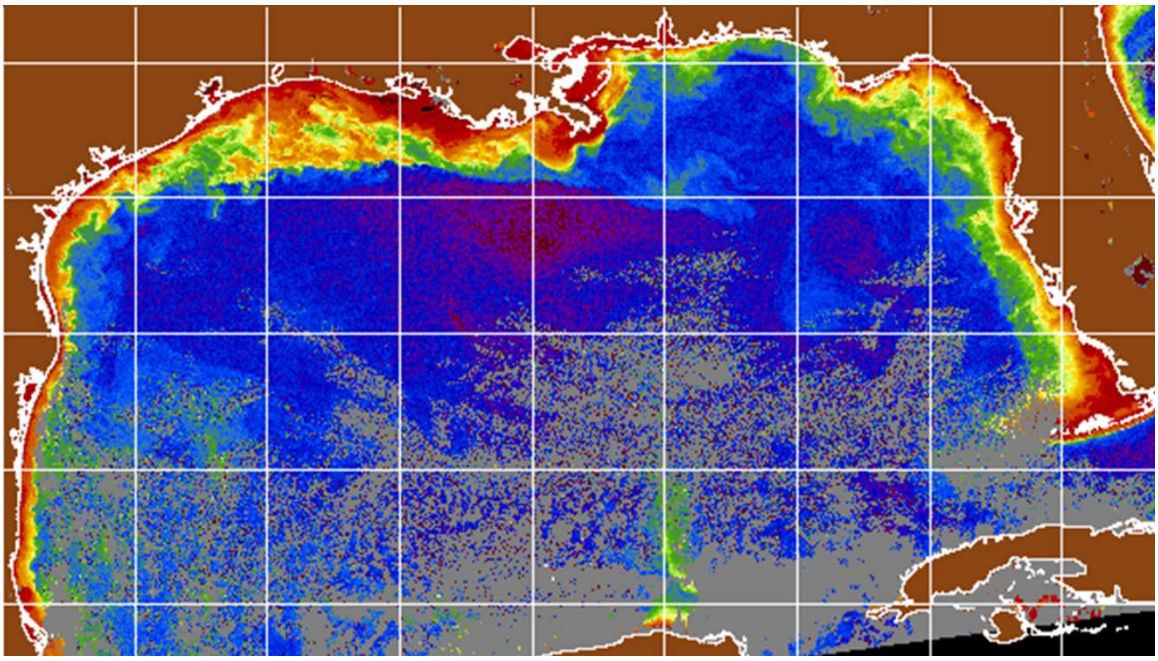

Figure 42 shows the horizontal visibility product from 25 Oct 2014 calculated using the VIIRS image and the LMI algorithm after regional adjustments were made. The maroon colored areas indicate algorithm failure. The updated coefficients clearly increase the number of valid retrievals in the coastal waters.

3.6 Image Merge

Image merge combines data from multiple satellites allowing enhanced spatial coverage by providing imagery from multiple look angles and small temporal differences. It is currently set up for merging MODIS and VIIRS Level-3 HDF4 files[8]. Figure 43 demonstrates the image merge capability included in AOPS v4.12. Often times, passive imagery is limited by environmental effects such as glint or clouds. The ability to combine individual images from different sensors can provide the ability to expand the product's field of view. This example combines the MODIS and VIIRS vertical visibility imagery to produce the merged product off west South Africa, 1 Feb 2015. There is very strong agreement between the initial images. Once merged the final product provides greater spatial coverage of vertical visibility for the area. This capability was tested for a variety of products and locations, Arabian Gulf results are shown in Figure 44. As not all imagery is suited for merging, a remote sensing subject matter expert is required to make final determination of product viability.

[8] In the future this capability will be made more flexible so additional sensors / products can be selected by user and provide the ability to merge Level-4 composites, including daily and 8 day rolling composites.

New AOPS v4.12 Sensor Merge Capability for MODIS/VIIRS

Example: Western South Africa – February 01, 2015

Vertical Visibility : Good Agreement

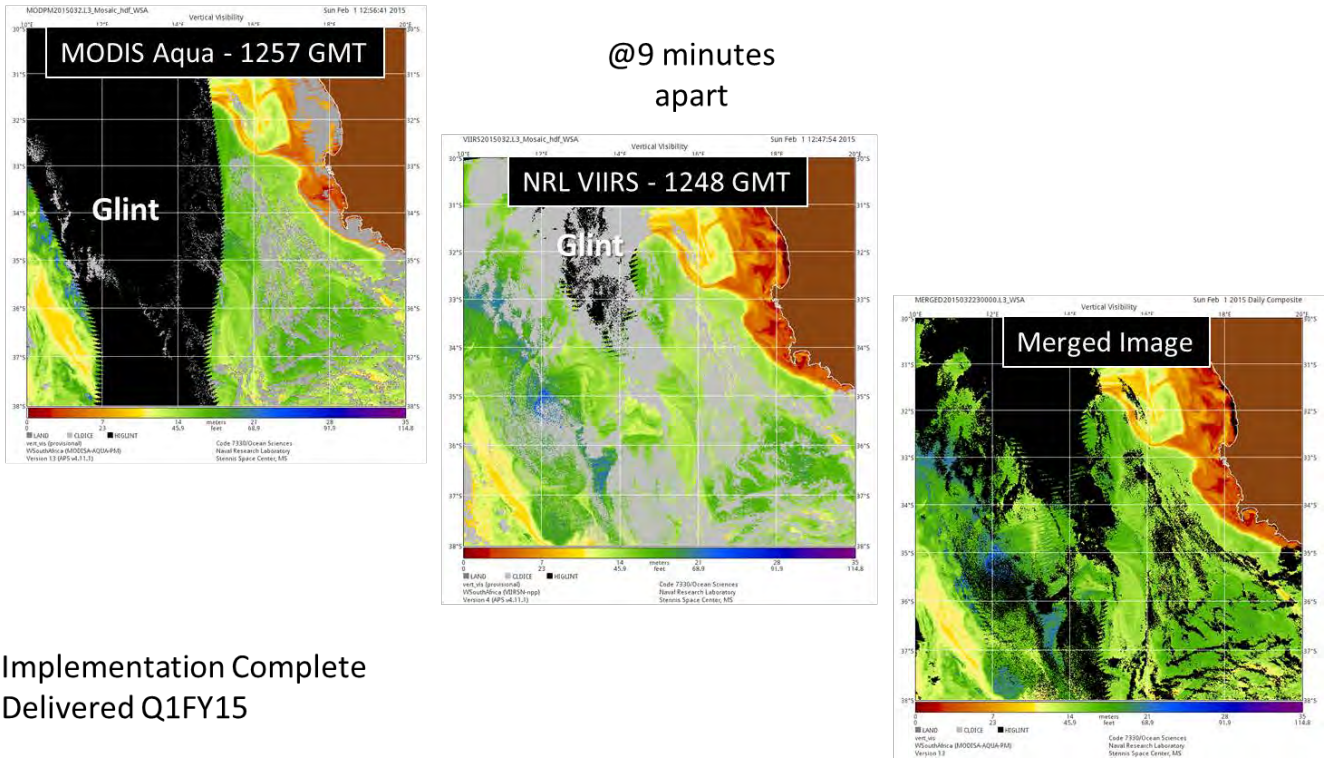

Figure 43 demonstrates the image merge capability included in AOPS v4.12**. Often times, passive imagery is limited by environmental effects such as glint or clouds. The ability to combine individual images from different sensors can provide the ability to expand the product's field of view. This example combines the MODIS and VIIRS vertical visibility imagery to produce the merged product off west South Africa, 1 Feb 2015. There is very strong agreement between the initial images. Once merged the final product provides greater spatial coverage of vertical visibility for the area.**

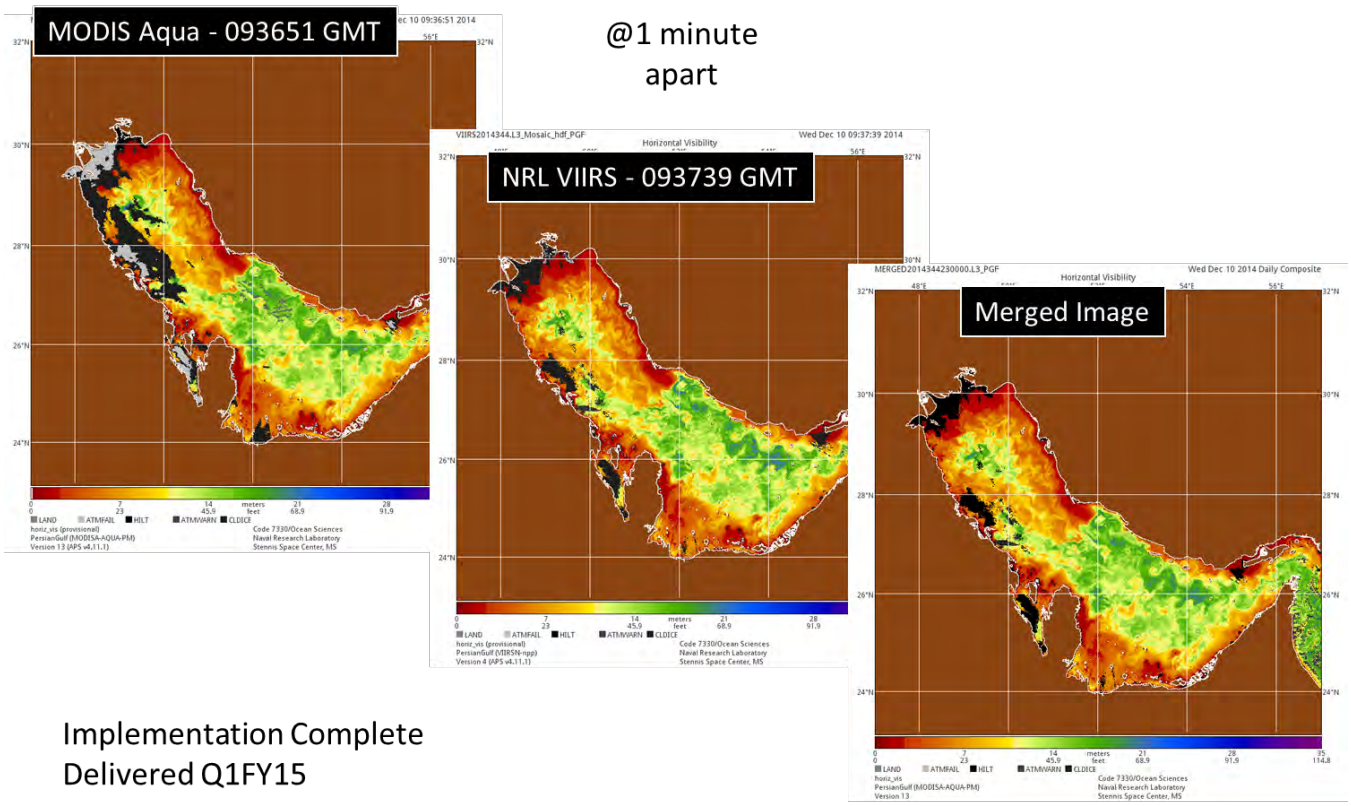

Figure 44 shows the image merge capability using the horizontal visibility products from the Arabian Gulf. MODIS and VIIRS images were taken approximately a minute apart and the process results shows strong agreement in the merged product.

4 Operational Implementation

4.1 Operational Concept

The system will reside with NP3 at the Naval Oceanographic Office and automatically produce near real time (NRT) ocean color products from several satellites. Multiple real time satellite data streams (NPP-VIIRS, MODIS-Aqua, GOCI) of SDR (level 1) will be automatically processed, *via AOPS v4.12*, into Navy ocean optical products. Products produced by NAVOCEANO will support fleet operations and internal modeling efforts. Initial testing efforts have shown that approximately 1.25 hours are required to receive VIIRS data from AFWA therefore an operational goal of approximately 2 hours to produce final products is reasonable.

Note: NAVOCEANO will not be pulling EDR's for Ocean Color as they intend to use the Navy algorithms to support operations.

4.2 Resource Requirements

Additional storage space on the A2 cluster and the SAN have been previously scoped out and additional capacity has been addressed during the JPSS/NPOESS system upgrades at NAVOCEANO.

4.3 Future Work

- Maintain current operational sensors:
  - Perform quarterly Cal/Val updates via the semi-automated "on-orbit vicarious calibration" technique for MOBY and WaveCIS. This activity will also provide insight necessary to define the uncertainty of the inter-sensor products.
  - Perform VIIRS SDR calibration update due to LUT changes and Delta-c implementation (awaiting time to acquire 20-40 high quality data collections) -- including upgrade and testing of core processing software (n2gen / NASA L2gen annual updates)
  - Monitor operational sensors at MOBY and AERONET-OC sites to insure data reliability
  - Maintain and monitor WaveCIS AERONet-OC data stream
  - Provide enhancements to large area / basin scale processing
  - Automated mapping and area of interest configuration
  - Improve efficiency of HDF input/output modules
  - Provide automated area coverage locator based on latitude and longitude as defined by user input
- Expand and transition initial AOPS capability to include use of Sentinel 3 and GOCI-2 for operational products,
  - acquire proxy data for pre-launch preparation and initial implementation into AOPS
  - evaluate future ocean color sensors for AOPS initial integration (GCOM SGLI (2016) and Sentinel-3B OLCI and JPSS VIIRS (2017))
- Finalize GOCI implementation and complete evaluation for operational use
- Final improvements and evaluation of sensor merge capability
- NexSat VIIRS NRT for Monterey/JPSS program (chl, SST, IOPs)
- Full implementation of sharpening using the VIIRS I-Bands within AOPS, *via C-code*; currently this capability works in conjunction with AOPS
- Improvements to the AOPS mosaicking capability
- Prepare the NRT Geostationary Ocean Color Imager (GOCI) data stream for integration into operations.
- Improvements in sensor characterization and algorithm development will be addressed as new versions of AOPS are transitioned to NAVOCEANO.

5 Summary and Conclusions

The Navy's assessment of the Visible Infrared Imager Radiometer Suite (VIIRS) on Suomi National Polar-orbiting Partnership (NPP) indicates the ocean color products are of high quality and ready for

operational use. Evaluations to date indicate that with vicarious calibration, the NOAA SDR meets Navy requirements for operational ocean optical products as demonstrated by comparison to both *in situ* data and Moderate Resolution Imaging Spectroradiometer (MODIS) products. The VIIRS and MODIS Navy algorithms are comparing very well, better than ever. In working with the JPSS CalVal Team we have seen that AOPS results (*spectral nLw*) show no significant discrepancies from products produced by NASA and NOAA.

Spatial and temporal variability of bio-optical properties combined with differences in measurement techniques and algorithms all contribute to inconsistencies between remotely sensed and *in situ* measurements. We provided ground truth measurement for several ocean color sensors, VIIRS, MODIS, and GOCI at several sites around the world. Comparisons are shown for the various satellites and *in situ* measurements of nLw, Rrs, chl, a, b_b and c using standard bio-optical algorithms. The results show reasonable agreement between satellite and *in situ* measurements with discrepancies attributed to imperfect atmospheric corrections, uncertainties originating from sampling errors (including pixel to point matchups and including sea surface variations), temporal collection variability (satellite image acquisition versus *in situ* collection time) and natural bio-optical variability at matchup location.

Gain monitoring showed the VIIRS sensor has not quite achieved stability. The gain over time should exhibit no trend. In light of the fact that a trend *(Figure 4)* is evident, periodic vicarious calibration will be required to make necessary adjustments in order to provide reliable real-time data needed to support naval operational use. Included in this VTR, we have provided updated vicarious calibration coefficients for VIIRS, MODIS and GOCI sensors using AOPS v4.12 processing. Matchup results demonstrated the coefficients improve the satellite performance as compared to *in situ* data and for cross platform evaluations.

The processing upgrades provided by AOPS v4.12 were shown to improve upon the previous AOPS v4.10 capabilities. Inter-sensor *(image to image)* comparisons show obvious improvements in image quality -- that in turn directly translate to improved product quality. A quantitative assessment looking at the error distribution between AOPS v4.12 and AOPS v4.10 shows that AOPS v4.12 has lower errors when compared to the same imagery processed with v4.10.

We looked at overall trends of the VIIRS ocean color matchups as compared to the blue water MOBY and green water WaveCIS ground truth stations. Time series and regression analyses showed VIIRS retrievals are satisfactorily reproducing the ground truth signal at all wavelengths. In blue waters, the strength of the regression is stronger at shorter wavelengths (blue-green) as expected, *primarily due to higher signal to noise and sensor sensitivity in that environment*. Conversely green waters show stronger correlation at the longer wavelengths (green - red). This is as expected due to the higher reflectance signals in the green and red wavelengths in the coastal environment, while the blue wavelengths (*especially 410 nm*) exhibit increased uncertainty due to variability in the atmospheric components and in water constituents. The matchup analysis of derived products provided acceptable results as well, with somewhat increased uncertainty due in part to algorithm limitations.

A vicarious calibration was performed for GOCI using select high quality MODIS scenes to synthesize ground truth stations at sites in the Sea of Japan. To evaluate GOCI we provided an inter-sensor

comparisons between GOCI, MODIS, and VIIRS products in the Yellow Sea as well as limited matchups (*n=12 in 2014*) with data from the AERONET-OC IEODO station. The gains provided with this VTR for GOCI were shown to improve reflectance retrievals and produce more reliable Navy products when compared to MODIS and VIIRS. Most reflectance and derived products showed the sensor is returning reasonable results. Unfortunately, a significant number of *in situ* matchups were not available as the IEODO system has not yet reached the maturity level of other AERONET-OC locations therefore; additional data is needed to define the accuracy and uncertainty of the GOCI ocean color products as well as the uncertainty of the *synthetic* vicarious calibration.

This VTR has demonstrated several new and upgraded capabilities. A procedure for the spatial enhancement of ocean color products was developed for VIIRS. The comparison of satellite products at 375-m and 750-m spatial resolution with *in situ* measurements of water leaving radiance and bio-optical properties showed that the 375-m products provide improved ability to resolve optical features in complex and rapid changing turbid environments such as the Chesapeake Bay and Mississippi River Plume. Upgrades to the LMI were shown to improve IOP determinations therefore allowing derivation of optical products at the 531 nm wavelength, yielding consistent diver visibility products from multiple sensors having unique spectral responses. Additionally, the image merge capability was delivered to enable fusion of data from multiple satellites providing enhanced spatial coverage through multiple look angles, *also minimizing the number of products sent out to fleet*.

Based on validation results, we recommend proceeding with operational processing of VIIRS sensor data using the Navy's Automated Optical Processing System (AOPS), *which is based on the NASA L2gen code for ocean color products*. Although continued sensor degradation and stability monitoring will be required, the products should provide an adequate follow-on and replacement to MODIS to support naval operations. The Navy sees no reason that the VIIRS sensor should not provide scientific research quality data for new algorithm development and the capability to produce operational products to support the fleet as well as perform ecological monitoring in global ocean waters. The GOCI sensor shows promise and can currently be used to support descriptive ocean analysis. We will continue efforts to monitor performance and uncertainty of GOCI in order to prepare it's imagery for integration into operations.

6 Acknowledgements

We would like to acknowledge the support of our Navy sponsors as well as our NOAA and NASA colleagues. The efforts and shared knowledge from the JPSS Cal/Val team, coordinated by Dr. Menghua Wang, have been invaluable in understanding VIIRS performance. We greatly appreciate the academic inputs and continuous processing improvement efforts and upgrades from the entire NASA OBPG team. We recognize the ongoing data collection efforts of Dr. Ken Voss and the MOBY team, Dr. Bill Gibson and Dr. Alan Weidemann for their efforts collecting the WaveCIS AERONET-OC data, as well as Dr. Giuseppe Zibordi and all of the AERONET researchers. A special thanks to Drs. Giulietta Fargion and Zibordi for assistance with developing protocols for using the L1.5 AERONET-OC data to support our near real time validation efforts. We thank Dr. Michael Ondrusek (NOAA/STAR) and Dr. Zhongping Lee (UMB) for the field data collected from the GEOCAPE and Chesapeake Bay cruises. We appreciate the organization efforts of NAVOCEANO *(VIIRS SDR via AFWA and GOCI SDR via MOA with Korea)*, NOAA CLASS and NASA for providing VIIRS, MODIS Aqua and GOCI imagery.

7 Technical References

Ahmed S, Gilerson A, Hlaing S, Weidemann A, Arnone R, Wang M. (2013) *Evaluation of ocean color data processing schemes for VIIRS sensor using in-situ data of coastal AERONET-OC sites* Proc. SPIE Vol. 8888: Remote Sensing of the Ocean, Sea Ice, Coastal Waters, and Large Water Regions.

Arnone R, Fargion G, Martionolch P, Ladner S, Lawson A, Bowers J, Ondrusek M, Zibordi G, Lee ZP, Trees C, Davis C, Ahmed S. (2012) *Validation of the VIIRS Ocean Color*, Proc SPIE, V 8372 Ocean Sensing and Monitoring IV.

Arnone R, Ladner S, Fargion G, Martionolch P, Bowers J, Lawson A. (2013) *Monitoring bio-Optical Processes Using NPP-VIIRS and MODIS-Aqua Ocean Color Products,* Proc. SPIE, 87240 Ocean Sensing and Monitoring V.

Arnone R, Vandermeulen R, Ladner S, Bowers J, Martinolich P, Fargion G, Ondrusek M. (2014) *Sensitivity of calibration gains to ocean color processing in coastal and open waters using ensembles members for NPP-VIIRS,* Proc SPIE Volume 9111: Ocean Sensing and Monitoring VI.

Bailey SW and PJ Werdell. (2006) *A multi-sensor approach for the on-orbit validation of ocean color satellite data products*, Rem. Sens. Environ. 102, 12-23.

Bailey, SW, Hooker SB, Antoine D, Franz BA, and Werdell PJ. (2008) *Sources and assumptions for the vicarious calibration of ocean color satellite observations,* Applied Optics, v 47, p2035.

Bowers J, Arnone R, Ladner S, Fargion G, Lawson A, Martinolich P, Vandermeulen R. (2014) *Regional vicarious gain adjustment for coastal VIIRS products*, Proc SPIE, Volume 9111: Ocean Sensing and Monitoring VI.

Brown SW, Stephanie JF, Feinholz ME, Yarbrough MA, Houlihan T, Peters D, Kim YS, Mueller JL, Johnson BC and Clark DK. (2007) *The Marine Optical BuoY (MOBY) radiometric calibration and uncertainty budget for ocean color satellite sensor vicarious calibration,* SPIE Europe Remote Sensing.

Chang C, Gould R. (2006) *Comparison of optical properties of the coastal ocean derived from satellite ocean color and in situ measurements*, Optics Express v 14 No 22, 10149.

Clark D, Murphy M, Yarbrough M, Feinholz M, Flora S, Broenkow W, Johnson BC; Brown S; Kim YS, Mueller J. (2003) *MOBY: A Radiometric Buoy for Performance Monitoring and Vicarious Calibration of Satellite Ocean Color Sensors: Measurements and Data Analyses Protocols*, Ocean Optics Protocols for Satellite Ocean Color Sensor Validation, Revision 4, Part VI, NASA Tech. Memo. 2003-210004/Rev 4./Vol. VI, NASA Goddard Space Flight, Greenbelt, Maryland, 3-34.

D'Alimonte D, Zibordi G, Mélin F. (2008) *A statistical method for generating cross-mission consistent normalized water leaving radiance,* IEEE Trans. Geosci. Remote Sens., v46, p 4075.

D'Alimonte D., Zibordi G. (2006). *Statistical assessment of radiometric measurements from autonomous systems,* IEEE Geosci. Remote Sens., v 44, p719.

Davis C, Tufillaro N, Nahorniak J, Jones B, Arnone R. (2013) *Evaluating VIIRS ocean color products for West Coast and Hawaiian waters* Proc SPIE, Baltimore Security and Defense Conference DS211 Ocean Sensing and Monitoring V.

Franz B, Bailey S, Werdell J, and McClain C. (2007). *Sensor-independent approach to the vicarious calibration of satellite ocean color radiometry.* Applied Optics, v 46, p5068.

Hoge FE and Lyon PE. (1996), Satellite retrieval of inherent optical properties by linear matrix inversion of oceanic radiance models: An analysis of model and radiance measurement errors, J. Geophys. Res., 101(C7), 16631–16648.

Hooker SH. McClain C, Mannino A. (2007) *A Comprehensive Plan for the Long-Term Calibration, and Validation of Oceanic Biogeochemical Satellite Data*, NASA/SP-2007-214152, 1-40pp.

Ladner S, Arnone R, Vandermeulen R, Martinolich P, Lawson A, Bowers J, Crout R, Ondrusek M. (2014) *Inter-Satellite Comparison and Evaluation of Navy SNPP-VIIRS and MODIS-Aqua Ocean Color Properties*, Proc SPIE, Volume 9111: Ocean Sensing and Monitoring VI.

Ladner S, Arnone R, Gould R, and Martinolich P. (2002) *Evaluation of SeaWiFS optical products in coastal regions*, Sea Technology v 43, p 29.

Lee Z, Hu C, Arnone R, and Liu Z. (2012) *Impact of sub-pixel variations on ocean color remote sensing products*. Optics Express, 20, 20844-20854.

Ondrusek M, Stengel E, Rella M, Goode W, Ladner S, Feinholz M, (2014) *Validation of ocean color sensors using a profiling hyperspectral radiometer*, Proc SPIE, Volume 9111: Ocean Sensing and Monitoring VI.

Pahlevan N, Lee Z, Lawson A, Arnone R, (2013) *Scene-based cross-comparison of SNPP-VIIRS and Aqua-MODIS over oceanic waters*, Proc. SPIE Vol. 8866, Earth Observing Systems XVIII.

Vandermeulen R, Arnone R, Ladner S, Martinolich P. (2015, *In Press*) *Enhanced satellite remote sensing of coastal waters using spatially improved bio-optical products from SNPP-VIIRS*. Remote Sensing of the Environment – RSE.

Wang M, Li X, Jiang L, Son S, Sun J, Shi W, Tan C, Naik P, Mikelsons K, Wang X, Lance V. (2014) *Evaluation of VIIRS ocean color products*, Proc SPIE Vol. 9261, Ocean Remote Sensing and Monitoring from Space.

Zibordi G, Holben B, Slytsker I, Giules D, D' Alimonte D, Milin F, Berthon J, Vandemark D, Feng H, Schuster G, Fabbri B, Kaitala S, and Seppala J. (2009) *AERONET-OC: A Network for the Validation of Ocean Color Primary Products*, Journal of Atmospheric and Oceanic Technology v 26, p1634.

8 List of Acronyms

Aerosol Optical Thickness (AOT)
Aerosol Robotic Network- Ocean Color (AERONET-OC)

Air Force Weather Agency (AFWA)
Anti-Submarine Warfare (ASW)
Automated Optical Processing System (AOPS)
Calibration and validation (Cal/Val)
Communication Ocean and Meteorological Satellite (COMS)
Comprehensive Large Array-data Stewardship System (CLASS)
Department of Defense (DOD)
Department of the Navy (DON)
Environmental Data Records (EDRs)
Expeditionary Warfare (EXW)
Geostationary Ocean Color Imager (GOCI)
Gulf of Mexico (GOM)
Hierarchical Data Format (HDF)
Integrated Data Processing System (IDPS)
Japanese Ocean Color and Temperature Sensor (OCTS)
Joint Polar Satellite System Suomi National Polar- Partnership (JPSS-NPP)
Joint Polar Satellite System (JPSS)
Korea Ocean Research and Development Institute (KORDI)
Level 2 generator (L2Gen)
Look up table (LUT)
Marine Optical Buoy (MOBY)
Medium Resolution Imaging Spectrometer (MERIS)
Meteorology and Oceanography (METOC)
Mine Warfare (MIW)
Moderate Resolution Imaging Spectrometers (MODIS on Aqua)
National Aeronautic and Space Administration (NASA)
National Center for Supercomputer Applications (NCSA)
National Oceanic and Atmospheric Administration (NOAA)
National Polar-orbiting Observation Environmental Satellite System (NPOESS)
Naval Oceanographic Office (NAVOCEANO)
Naval Research Laboratory (NRL)
Naval Special Warfare (NSW)
Near infrared (NIR)
Near real time (NRT)
Normalized water leaving radiance (nLw)
Ocean Biology Processing Group (OBPG)
Ocean Colour Monitor (OCM)
Polarization Detection Environmental Radiometer (POLDER)
Quasi-Analytical Algorithm (QAA)
Red Hat Enterprise Linux (RHEL)
Rrs Remote sensing reflectance
SAVANT - Satellite Validation Navy Tool (SAVANT)
Scientific Data Record (SDR)
Sea-viewing Wide Field-of-view Sensor (SeaWiFS)
Space and Naval Warfare Systems Center (SPAWARSYSCEN)
Top of atmosphere (TOA)
Validation Test Report (VTR)
Visible Infrared Imager Radiometer Suite (VIIRS)

9 Appendix

9.1 Overview of OBPG on-orbit vicarious calibration technique

The current procedure for ocean color Cal/Val following the OBPG approach (Figure 45) requires several years of coincident satellite and high quality *in situ* data before applying calibration gains and

sufficient matchups to produce algorithm validation[9] (Bailey and Werdell, 2006). The vicarious adjustment calculations (calibration) are performed using *in situ* spectral radiance propagated to Top of Atmosphere (TOAv) for each satellite to form a ratio ("gain") with the spectral TOAs of the satellite using the standard atmospheric correction of Gordon/Wang (1994) with a NIR iteration (Stumpf, et. al) assuming perfect sensor calibration in the NIR channels. The process begins by performing the initial atmospheric correction of the input VIIRS Lt to obtain the nLw at the point in question. The various atmospheric components (Lr, La, transmittances, etc.) and pointing-angles are saved during this process. nLw is then replaced with the in-situ (convolved MOBY or hyper spectral model shifted AERONET) derived values. The atmospheric components are added to the replaced nLw to obtain a new Lt from the view of the VIIRS. This new Lt is known as the vicarious Lt (vLt). In a perfect system in which all components are computed accurately, the vLt and original Lt should have a ratio of 1.0.

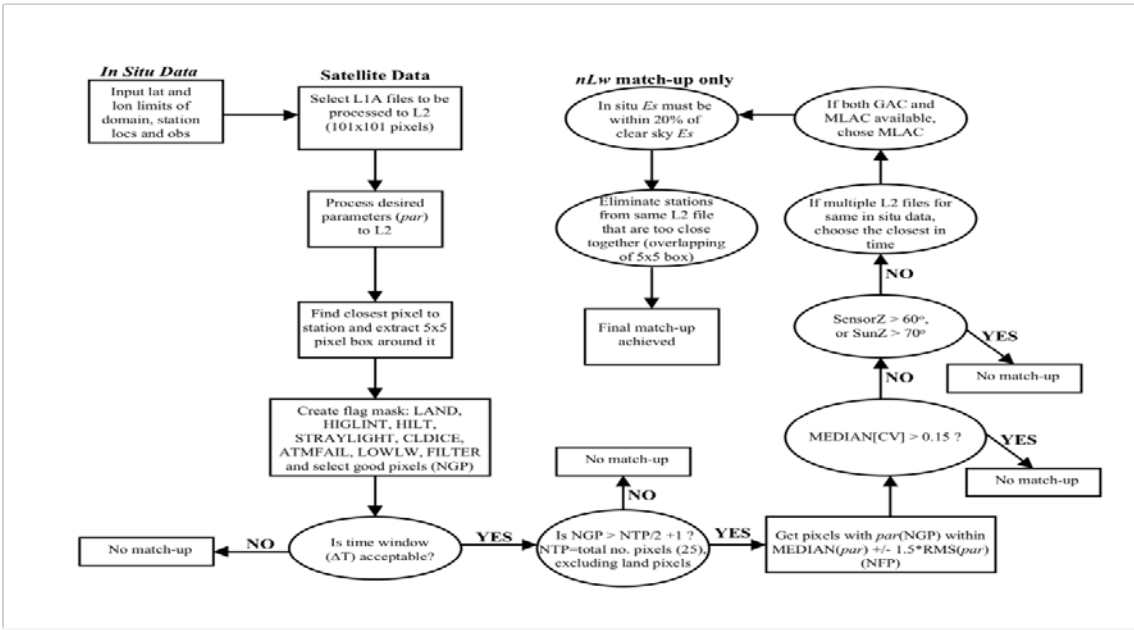

Figure 45 Match-up procedure for comparing *in situ* and satellite data employed by NRL is similar to that used by NASA OBPG.

9.2 Pareto Chart Procedure

1) Determine relevant binning categories, *used for grouping results.* Here we are interested in the frequency of occurrence of data within a given error from the MOBY buoy. We want to see how much data is within 5% of MOBY and 10% and so forth. Therefore we use 5% increments up to the 20% error, then 10% increments up to 50% error and ultimately grouping everything over

[9] Over 9-years, MOBY provided about 1450 contemporaneous match ups for SeaWiFS and only 150 match-ups passed the stringent screening processes for long-term vicarious calibration (*approximately 17 per year*). BOUSSOLE Project information is available at http://www.obs-vlfr.fr/Boussole/

50.01% error together [0 -5%, 5.01-10%, 10.01-15%, 15.01% -20%, 20 – 30%, 30 – 40%, 40 – 50%, >50.01%]

2) Decide what period of time the Pareto chart will cover. We use June 2012 – Dec 2014; dates prior to May 2012 had major LUT upgrades and other SDR implementations leading to improved SDR products[10].
3) Assemble the data.
4) *We used the Histogram feature with Pareto Chart (not sorted) in MS Excel for the following steps*
   a) Subtotal the measurements in each category.
   b) Determine the appropriate scale for the measurements and express the maximum value, n = total number of matchups
   c) Construct bar chart.
   d) Calculate the percentage for each category: the subtotal for that category divided by the total for all categories. Shown on a right vertical axis and labeled with percentages. *Note, the two scales match: For example, the left measurement that corresponds to one-half should be exactly opposite 50% on the right scale.*
   e) Calculate and display on the second y-axis the cumulative sums as a percent of the total. For the first category, # of matchups/total # samples, then add the subtotals for the first and second categories, and put a marker over the second bar indicating that sum. To that sum add the subtotal for the third category, and mark over the third bar for that new sum. Continue for all the categories/bars. Note: the last marker should reach 100 percent on the secondary y axis.

[10] *Another major system upgrade was made at the SDR level in May 2014. It is referred to as the* Delta-c *implementation (bias constant in polynomial is set to zero). As data accumulates this will need to be considered in future assessments as post* Delta-c *data will likely have different gain factors.*

9.3 Calibration and Validation Process

In situ bio-optical global and coastal measurements have a critical function in satellite calibration/validation (Cal/Val) activities, the development of remote-sensing algorithms and statistical models that convert radiometric measurements *(water leaving radiance or surface reflectance)* to geophysical data products *(chlorophyll a and others)*. The quality of these Cal/Val and conversion algorithms cannot be better than that of the data sets of ocean properties used to create them.

In situ data collected for Cal/Val uses the same measurements and methodologies, but calibration requires data with lowest possible measurement uncertainty. Functionally this means that calibration sites must be selected such that they exhibit minimal natural (oceanic and atmospheric) variability (Hooker et al., 2007). Today the ocean color community views *in situ* data as having variable quality, and therefore these data should be ranked by quality for different purposes (from highest quality to lowest): calibration, validation/algorithm development, general research, and monitoring. Guidelines for calibration/validation (Cal/Val) field programs are:

1. Data collected in a stable environment (spatially & temporally homogeneous; and known atmospheric conditions) and sufficiently far from land (>5km);
2. Sample all measurements necessary to produce good water leaving radiance data. Measurements should have well defined uncertainties quantified, collected with appropriate methodologies (approved protocols), with calibrated instruments (pre/post-cruise calibrations that are traceable). Cal/Val team should define set of parameters to be measured to have cross-site consistency;
3. Sample as close to satellite overpass as possible, preferably in a time-series. Continuous data will have higher match-up retrievals and will allow for assessment of products for successive missions and ability to define temporal and spatial uncertainty in measurements;
4. Globally distributed *in situ* data to fully represent the wide range of geophysical conditions that remote sensing is expected to observe; and
5. Consistent data processing with a clear QA/QC process.

MOBY and BOUée pour l'acquiSition d'une Série Optique à Long termE (BUSSOLE) buoys are the primary Cal/Val sites and both comply with the above calibration guidelines.[11]

However, we are able to facilitate the operational use of VIIRS by using both open ocean and coastal Cal/Val sites and making minor modifications to existing methodology: primarily point one above and the exclusion criteria currently used by the NASA Ocean Biology Processing Group (OBPG), *refer to Appendix 9.1*. Real time coastal sites, though of lower quality, have been successfully used to monitor sensor stability and provide sufficient “matchups” in real time to perform more routine updates of the vicarious calibration.

[11] These buoys have been the primary basis for the on-orbit vicarious calibrations of the USA Sea-viewing Wide Field-of-view Sensor (SeaWiFS), the Japanese Ocean Color and Temperature Sensor (OCTS) and Global Imager (GLI), the French Polarization Detection Environmental Radiometer (POLDER), the USA Moderate Resolution Imaging Spectrometers (MODIS, Terra and Aqua), the Japanese Global Imager (GLI), and the European Medium Resolution Imaging Spectrometer (MERIS).

The Satellite Validation Navy Tool (SAVANT) provides NRL with a semi-automated and near-real-time capability for performing flexible validation match-up analysis following the NASA OBPG procedures and monitoring capability for satellite performance. For validation match-ups, we use the AERONET sites (nLw, Level 1.5) and the satellite (Level 3). The satellite spatial box can be set to a single pixel, or 9 km^2 or 25 km^2 centered on the *in situ* data collection platform (*latitude, longitude*). Exclusion criteria which can be set in SAVANT are:

- The time window can be set to define coincident as ± 1hr to ± 3 hours, in 30 minute increments.
- *In situ* data are typically screened as follows:
    - exclude wind speeds > 8 m/s
    - set a maximum Aerosol Optical Thickness (AOT) = 0.2
    - set the minimum nLw value = 0
    - set the maximum nLw value = 3
- Satellite data can be screened as follows:
    - set the maximum Coefficient of Variance = 0.30
    - set the minimum percent valid pixel requirement to 50
    - set the satellite box size = single pixel, 9 km (3 km x3km AOI) or 25km (5 km x5 km AOI)
    - set the satellite zenith angle minimum = 0 and maximum = 56
    - set the solar zenith angle minimum = 0 and maximum = 70
    - set the satellite azimuthal angle minimum = -180 and maximum = 180
    - set the solar azimuthal angle minimum = -180 and maximum = 180
- The Level 2 quality flags that can be applied to satellite data allows exclusion of scenes affected by: atmospheric failure, high LT (saturation), could/ice, low water-leaving radiance, land, high satellite zenith angle, high solar zenith angle, navigation failure, high glint, stray light, maximum NIR iteration reached, high polarization, and moderate sun glint.

The technical details of development and implementation are also provided in the Space and Naval Warfare Systems Command (SPAWAR) FY2013 and FY2014 Monthly Progress Reports, and the originating vicarious calibration papers written by Franz et al., 2007 and Bailey et al., 2008.